SYNTHESIS AND CHARACTERIZATION OF ALUMINUM DOPED TO EXTEND CATHODE LIFE IN LI-ION BATTERIES

A Thesis Submitted to
The Graduate School of Engineering and Science of
İzmir Institute of Technology
in Partial Fulfillment of the Requirements for the Degree of

MASTER OF SCIENCE

in Chemistry

by
Onur TEKİN

July 2021
İZMİR

ACKNOWLEDGMENTS

There are many people whom I owe thanks in the course of my work. First of all, I would like to thank my thesis advisor Associate Professor Engin Karabudak for his experiences, guidance, teacher-student relationship he shared with me, as well as for always approaching me as a friend.

In addition, I would like to thank Associate Professor Ümit Hakan Yıldız and Associate Professor İbrahim İnanç, the other members of my thesis committee, for the valuable information they shared with me, their opinions and suggestions.

I would also like to thank Yusuf Emre Göl and Ahmet Aytekin, who are members of the Karabudak research group, who helped me during my research and experiments.

I would like to thank my classmate and roommate Turgut Uğur, who has endured all difficulties with me for six years. I would like to thank my classmates Hazal Tosun, Buse Tütüncü, Miray Cebeci and Sümeyra Sözer, who shared all their good and bad memories with me and studied for exams when appropriate.

Finally, I would like to express my gratitude and love to my mother, father and brother Nilüfer Tekin, Birol Tekin and Cihan Tekin, who have never ceased to support me throughout my education life and have constantly worked hard to build a better future for me.

ABSTRACT

SYNTHESIS AND CHARACTERIZATION OF ALUMINUM DOPED TO EXTEND CATHODE LIFE IN LI-ION BATTERIES

Lithium-ion batteries have an important place in meeting the energy needs and are of greater importance than their cognates, thanks to their characteristics as secondary batteries. Volumetric and gravimetric energy densities are the main features that carry lithium-ion batteries to the top. Lithium-ion batteries consist of different parts: cathode, anode, separator and electrolyte. While the anode materials are generally based on silicon, carbon and tin, the cathode materials include layered $LiCoO_2$, spinel $LiMn_2O_4$, olivine $LiFePO_4$, layered $LiNi_{0,8}Co_{0,15}Al_{0,05}O_2$(NCA) and layered $LiNiCoMnO_2$ (NMC). Nmc and nca cathode materials stand out due to their high energy densities.

Of course, lithium-ion batteries also have some disadvantages. A prime example of this is the capacity reductions it experiences with the increasing number of cycles. The main reasons for the decrease in capacity are; The transformation of the layered structure into spinel structure, the contamination of the Lio structure on the cathode to the electrolyte structure as a result of the side reactions that occur, damage the stable structure of the electrolyte and lead to Li loss. Metal oxide surface modification methods come to the fore in studies conducted to prevent these disadvantages.

In this study, nmc structure was synthesized by reprecipitation method. Xrd, and sem analyzes of the obtained structure were taken. Al_2O_3 surface modification method was applied on the cathode surface. Cyclic voltammetry analyzes of the nmc structures with and without the modification applied were made with the help of potentiometry and the results were compared.

ÖZET

Lİ-İYON BATARYALARDA KATOT ÖMRÜNÜ UZATMAK İÇİN ALÜMİNYUM KATKILI MALZEMELERİN SENTEZİ VE KARAKTERİZASYONU

Lityum iyon bataryalar enerji ihtiyacını karşılamada önemli yer tutmaktadır ve ikincil bataryalar olma özellikleri sayesinde soydaşlarından daha büyük önem arz etmektedir. Volumetrik ve gravimetrik enerji yoğunlukları ise lityum iyon bataryaları zirveye taşıyan başlıca özellikleridir. Lityum iyon bataryalar, katot, anot , seperatör ve elektrolit olmak üzere farklı bölümlerden oluşur. Katot, pozitif elektrot olarak karşımıza çıkarken, anot ise negatif elektrot olarak adlandırılır. Anot malzemeleri genellikle silisyum, karbon ve kalay bazlı olmakla birlikte katot malzemelerinde ise katmanlı $LiCoO_2$, spinel $LiMn_2O_4$, olivin $LiFePO_4$, katmanlı $LiNi_{0,8}C_{o0,15}Al_{0,05}O_2$(NCA) ve katmanlı $LiNiCoMnO_2$ (NMC) örnek olarak gösterilebilir. Nmc ve nca katot malzemeleri yüksek enerji yoğunlukları sebebi ile öne çıkmaktadır.

Lityum iyon bataryaların elbette bazı dezavantajları da vardır. Artan çevrim sayısı ile birlikte yaşadığı kapasite düşüşleri buna başlıca örnektir. Kapasite düşüşünün başlıca sebepleri; katmanlı yapının spinel yapıya dönüşmesi, katot üzerindeki Lio yapısının, gerçekleşen yan reaksiyonlar sonucunda elektrolit yapısına bulaşması, elektrolitin kararlı yapısına zarar vermekle Li kaybına yol açar. Bunun sonucunda elektrolit yapısında gerçekleşen reaksiyonlar sonucunda HF asidinin katot yapısına zarar verdiği görülmektedir. Bu dezavantajları engellemek amacıyla yapılan çalışmalarda metal oksit yüzey modifikasyonu yöntemleri öne çıkmaktadır.

Bu çalışmada tekrardan çöktürme yöntemi ile nmc yapısı sentezlenmiştir. Elde edilen yapının xrd, ve sem analizleri alınmıştır. Katot yüzeyinde Al_2O_3 yüzey modifikasyonu yöntemi uygulanmıştır. Elde edilen modifikasyon uygulanmış ve uygulanmamış nmc yapılarının potansiyometri yardımı ile çevrimsel voltametrik analizleri yapılmış ve sonuçlar karşılaştırılmıştır.

TABLE OF CONTENTS

LIST OF FIGURES

Figure **Page**

LIST OF TABLES

Table **Page**

CHAPTER 1
INTRODUCTION

1. 1. Motivation of the study

From past to present, many different cathode materials have been researched, developed and used to serve many different purposes. When compared to other cathode materials, NMC cathodes stand out with their non-toxicity, low cost and high energy density. So much so that, thanks to these features, their use in all areas of today has become quite widespread and has put it as a candidate for the top. The best example of this; Tesla company, one of the largest and most successful companies in the world, prefers nca cathode and batteries as battery material in electric vehicle productions that dominate the market. In addition to the prominent features of the Nca cathode, the side reactions that occur on the surface during its use, the deterioration of the cathode material, and the shortening of its life can be given as examples. Our motivation in this study; The aim is to work on extending the life of the cathode and extending its stability.

1. 2. History of batteries

The first battery was invented in 1800 by Alexander Volta, who used zinc and copper discs in a NaCl solution (Volta 1800). In 1859, Gaston Plante produced the first rechargeable lead-acid battery, and in 1866, Georges-Lionel Leclanché developed the zinc-carbon battery, which was used as an anode in ammonium chloride solution and a mixture of manganese oxide-carbon as the cathode, which has survived to the present day. invented (Leclanche 1866). In 1899, Swedish engineer Waldmar Jungner invented the first nickel-cadmium battery. In 1901, Thomas Edison patented the nickel-iron battery. Later, batteries such as nickel-zinc, silver-zinc, nickel hydrogen and lithium batteries were developed in line with advancing technology and increasing needs (Linden 2002).

After G. N. Lewis made the first study of lithium batteries in 1912, lithium batteries could not be commercialized until the 1970s. The reason why lithium batteries came to the fore in the 1970s was the emergence of the need for portable energy in the military and medical fields. Studies on non-rechargeable lithium batteries, which were commercialized in the 1970s, increased rapidly in the 1980s. Explosions occurred in batteries using lithium metal as a result of heat release and thermal decomposition with exothermic reactions due to the contact of lithium metal with air, which forced researchers to find alternative electrode materials. In the studies, carbon-based materials were developed as the anode and lithium metal oxide materials were developed as the cathodes. In this way, even if there is a decrease in the energy density, the risk of explosion is made much lower. The first rechargeable lithium-ion battery was commercialized by Sony in 1991 with the work of John B. Goodenough and his team (Linden 2002).

After being commercialized in 1991, lithium-ion batteries started to be used especially in medical, military and portable electronic devices (mobile phones, electronic cameras and camcorders, laptop computers) due to their high energy density as well as their small and light weight. In addition, it is used in the storage of energy obtained from renewable energy sources and in electric vehicles that are expected to take the automotive industry under full control in the future. As a result, today, there is almost no house where lithium-ion batteries do not enter, and it is one of the most important sine qua non of advancing technology. The lithium-ion battery market, which approached 30 billion dollars in 2015, is expected to reach 77 billion dollars in 2024 with an annual growth of 12.5% . Lithium-ion batteries are one of the batteries with the highest share in the energy storage market and the most investments, with the widespread use of electric and hybrid vehicles (Pillot 2013). Although $LiCoO_2$, which was the first cathode material commercialized in 1991, is still used in consumer electronics, the use of this cathode material has decreased compared to its early days due to the expensive and toxic nature of cobalt. $LiFePO_4$s, which are safer cathode materials than LCO cathode materials, lagged behind LCO in terms of specific energy density. Li_2MnO_4 was used because of its high nominal voltage and $LiFePO_4$ because of its long cycle life (Chen, et al. 2011, Goodenough and Kim 2010). LFP is used in electric vehicles due to its long cycle life, while LCO is used in consumer electronics due to its high energy density. Finally, two new cathode materials, $LiNiCoAlO_2$ and $LiNiCoMnO_2$, which have high capacity and

nominal voltage, have been found and studies have been carried out especially for their use in electric vehicles (Nitta, et al. 2015).

Lithium-rich NMC cathode materials are one of the most concentrated cathode materials in the lithium-ion battery industry, where high investments are made. Lithium-rich NMC cathode materials have high capacity and energy density due to their ability to operate in the high voltage range (Rozier and Tarascon 2015).

1. 3. Lithium Ion Batteries

Lithium-ion batteries are secondary batteries, meaning they can be recharged. In addition to this feature, they have high energy density according to their weight and size. Because of these properties, they are used in fields such as military, medical, automotive and consumer electronics. When the gravimetric and volumetric energy densities of the secondary batteries are compared, it is seen in Figure 1.1 that the batteries with the highest both volumetric and gravimetric energy densities are lithium-ion batteries. The reason for these features of lithium-ion batteries is the use of lithium, which has the highest oxidation potential, the lowest atomic weight, and a specific capacity of 3680 Ah/kg according to the periodic table due to its electropositivity.

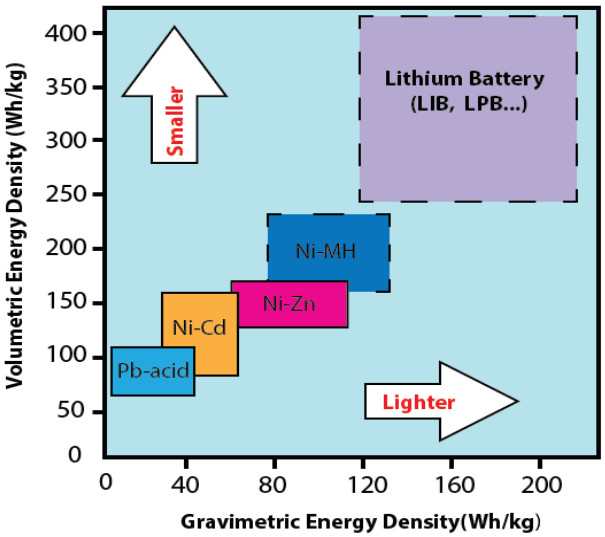

Figure 1.1. Secondary batteries in terms of gravimetric and volumetric energy density (Source:"Http://Www.Epectec.Com/Batteries/Cell-Comparison.Html")

Unlike other secondary batteries, lithium-ion batteries do not show a memory effect. In other words, when they are recharged without being fully discharged, there is no significant loss of capacity. When they are not used, the loss of capacity is very small and slow. At the same time, they do not require maintenance and do not harm the nature. On the other hand, lithium-ion batteries lose capacity in case of overcharge and degrade at high temperatures. In addition, the expensiveness of the materials used in the production of lithium-ion batteries is an important disadvantage (Linden 2002). The advantages and disadvantages of lithium-ion batteries are compared in Table 1.1.

Table 1.1. Advantages and disadvantages of Li-ion batteries

Advantages	**Disadvantages**
Rechargeability and High energy density	The use of expensive materials in its manufacture
Low intensity	Loss of capacity due to overcharging
Ability to operate in wide and high voltage range	Requires a protective circuit
Operation in wide temperature range	Thermal decomposition at high temperatures
High coulombic efficiency	Low level of security risks

(Cont. on next page)

Table 1.1(cont.)

Low memory effect and Fast charging	
Low capacity loss when not in use	
Maintenance free and Long shelf life	

1. 3. 1. Areas of use

Lithium-ion batteries are used in smart mobile phones, laptops, electronic tablets, digital cameras, video cameras, unmanned aerial vehicles (drones), smart watches and even wireless headphones, which are used by almost the whole world today. Lithium-ion batteries are one of the parts that enable all these electronic devices to be used in smaller sizes. Because while lithium ion batteries occupy a large place in these electronic devices, with the development of lithium ion battery technologies, lithium ion batteries have shrunk, so electronic devices have also shrunk. Another promising area of use for lithium-ion batteries is in electric vehicles. Electric vehicles, the production and use of which have increased rapidly in the last few years, are expected to completely replace vehicles with internal combustion engines in the future. This has increased investments in lithium-ion battery technologies. Lithium-ion batteries, which are also used in telecommunication, space applications, military and medical fields, are also used to store energy obtained from solar panels and wind turbines, that is, energy obtained from renewable energy sources. In the future, it will be possible to see automobiles, sea vehicles and even aircraft that operate with the energy obtained from renewable energy sources and use lithium-ion batteries. Usage areas of lithium-ion batteries are summarized in Figure 1.2.

Figure 1.2. Usage areas of lithium-ion batteries
(Source:http://www.pasticheenergysolutions.com/applications/).

1. 3. 2. Main components of lithium-ion batteries

The main components of lithium ion batteries are anode, cathode, separator and electrolyte. The anode is used as the negative electrode, the cathode is the positive electrode, the separator is used as the plate between the electrodes, and the electrolyte is used between the electrodes to provide ion transfer. The main components of lithium-ion batteries are shown in Figure 1.3.

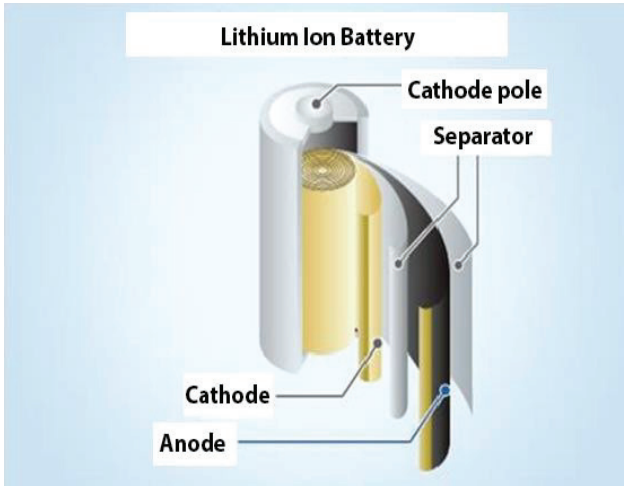

Figure 1.3. The main components of lithium-ion batteries.

(Source: Http://Www.Emc2.Cornell.Edu/Content/View/Battery-Anodes.Html)

1. 3. 2. 1. Anodes

The anode is used as a negative electrode in lithium ion batteries. In a rechargeable lithium-ion battery, the anode plays the role of negative pole during discharge and positive pole during charging ("Http://Www.Emc2.Cornell.Edu/Content/View/Battery-Anodes.Html"). Many anode materials such as lithium, carbon, silicon, tin-based materials as well as transition metal oxides have been used since the emergence of lithium-ion batteries ("Http://Www.Emc2.Cornell.Edu/Content/View/Battery-Anodes.Html"). Although pure lithium is used as an anode, it is not used much today, except for experimental studies, because it is expensive, creates safety risks and dendritic growth is observed. Instead of pure lithium, lithium aluminum alloys and lithium titanium oxide have been used as anode material. Lithium aluminum alloys, on the other hand, are not used much today due to the volume change that occurs during lithium ion displacement. Instead of these alloys, intermetallic compounds (such as Al_3Ni, FeSn, Sn-Sb, Sn-Cu) that can alloy with lithium such as aluminum, tin, cadmium, antimony, and bismuth and that cannot alloy such as iron, nickel, cobalt, and copper are used (Inoue and Zou 2005, Shukla 2008). Lithium titanium oxide ($Li_4Ti_5O_{12}$), another alternative anode material, does not undergo

volumetric changes during lithium ion displacement, but has limited use in applications requiring high energy density and high voltage (Hummel 2011).

Graphite, graphite oxide, graphene, soft carbon, hard carbon, carbon nanotubes, carbon nanowires and their composites are used as carbon-based materials. Graphite is one of the most commercially used carbon-based anode materials because of its low cost. The theoretical capacity of graphite is ~372 mAsa/g, and its irreversible capacity is ~330 mAsa/g. And also Lithium ions are easily incorporated into graphite and easily separated, forming a solid electrolyte interface (SEI) layer with electrolyte solutions. However, irreversible capacity losses are seen in lithium-ion batteries using graphite anodes. Hard carbon has a higher irreversible capacity than graphite and is cheaper than hard carbon graphite. Therefore, hard carbon is used commercially as much as graphite in lithium-ion batteries (de las Casas and Li 2012, Endo, et al. 2000, Yao and Cojocaru 2013).

The main reason why lithium ions can easily bind and detach from the structures of materials such as silicon (4200 mAsa/g) and tin (994 mAsa/g) and these materials cannot be used widely despite their high theoretical capacities is that they undergo volumetric changes during lithium ion displacement. The scientific community is working intensively to increase the tolerance of these materials, especially against volumetric change (Zhang 2011). Required properties of anodes used in lithium ion batteries

1. Volumetric change during the entrance and exit of the lithium ions into the structure

2. Lithium ions can easily enter and exit the structure

3. High initial capacity

4. High irreversible capacity,

5. High capacity conservation

6. Easy to produce

7. Being cheap

8. It has low reactivity towards electrolyte.

1. 3. 2. 2. Cathodes

The cathode is used as the positive electrode in lithium-ion batteries and takes the role of positive pole during discharge and negative pole during charging. Layered, spinel and olivine cathode materials are used commercially. They are generally in the form of lithium metal oxide or lithium metal phosphate. There are 5 basic cathode materials used today. These can be summarized as $LiCoO_2$ (LCO), $LiMn_2O_4$ (LMO), $LiFePO_4$ (LFP) $LiNiCoAlO_2$ (NCA), LiNiCoMnO2 (NMC). The crystal structures and electrochemical properties of these cathode materials are compared in Table 1.2.

Table 1.2: Structures and electrochemical properties of 5 basic commercial cathode materials

comparison of properties (Yuan 2013).

Cathode Material	Structure	Li/Li+ Rated Voltage (V)	Specific capacity (ms/g)	Specific Energy Density (Wsa/kg)
$LiCoO_2$	Layered	3,6	120-150	432-540
$LiMn_2O_4$ (LMO)	Spinel	3,8	100-135	380-520
$LiFePO_4$ (LFP)	Olivine	3,45	150-170	510-590
$LiNi_{0,8}Co_{0,15}Al_{0,05}O_2$ (NCA)	Layered	3,8	180-200	680-760
$LiNi_{0,5}Co_{0,2}Mn_{0,3}O_2$	Layered	3,8	160-190	610-730
$Li_{1,2}Ni_{0,2}Co_{0,08}Mn_{0,52}O_2$	Layered	3,7	220-260	820-970

$LiCoO_2$ was the first cathode material to be commercialized in 1991 and was used in consumer electronics, but the use of this cathode material has declined due to cobalt being expensive and toxic. Although the LFP, which emerged later on, were safer cathode materials, they could not exceed the LCO in terms of specific energy density. LMO stands out with its high nominal voltage and LFP with its long cycle life (Yuan 2013). LFP is used in electric vehicles due to its long cycle life, while LCO is used in consumer electronics due to its high energy density. In addition, new cathode materials were produced by making various additives to these materials.

Materials with good results such as $LiNi_{0,5}Mn_{1,5}O_4$ have been used. Finally, two new cathode materials, $LiNiCoAlO_2$ with high capacitance and rated voltage, and $LiNiCoMnO_2$ materials have been found and studies have been made especially for use in electric vehicles. Today, electric vehicles using these two cathode materials are increasing rapidly.

The features that should be in the cathodes used in lithium-ion batteries;

1. High initial capacity

2. Having high energy density

3. High irreversible capacity

4. The ability of a large number of lithium ions to be easily attached to the crystal structure

5. High capacity conservation

6. Ability to work in high and wide voltage range

7. Easy to manufacture

8.It is safe

9. Being harmless to the environment

10. It is low cost.

1. 3. 2. 2. 1. Layered cathode materials

$LiCoO_2$, which was the first cathode material to be commercialized and continues to be used effectively today, has an α-$NaFeO_2$ layered structure. The crystal structure of $LiCoO_2$ is shown in Figure 1.4. In addition, $LiNiO_2$ has the same structure as $LiCoO_2$, lower cost and higher capacity than $LiCoO_2$. However, it is not used much commercially because the thermal stability of LiNiO2 is low and its structure decomposes depending on the temperature (Demiray 2007). The structure of the layered $LiMO_2$s is generally shown in Figure 1.5.

The layered cathode materials in which the studies are accelerated and intense today are $LiNi_{0,8}Co_{0,15}Al_{0,05}O_2$ (NCA) and $LiNiCoMnO_2$ (NMC). These two cathode materials are used especially in electric vehicles thanks to their high capacities and high nominal voltages. NCA cathode materials are used in electric vehicles launched by the Tesla brand and stand out with their long life compared to cobalt-based batteries with high energy density. However, in NCA batteries, there are problems such as loss of capacity at high temperatures (40-70°C) due to the growth of the SEI layer and the growth of microcracks at the grain boundaries (Bloom, et al. 2003).

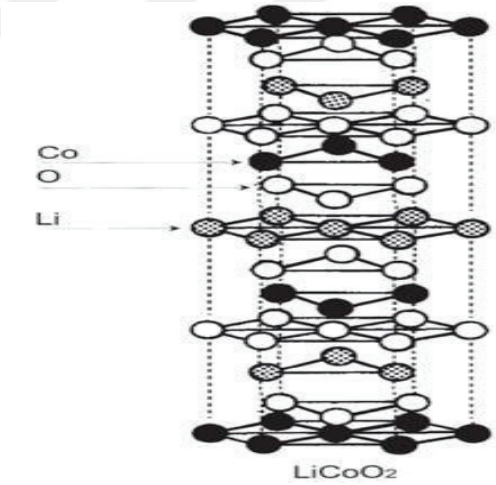

Figure 1.4. Crystal structure of layered $LiCoO_2$. (Source: Linden 2002).

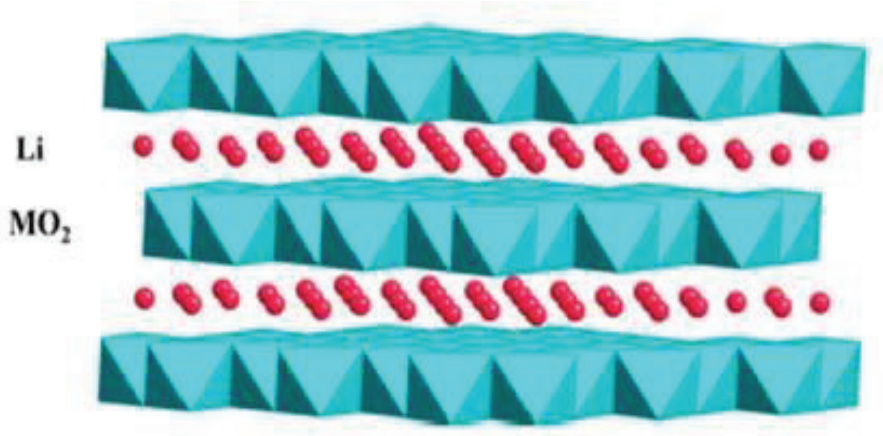

Figure 1.5. Representation of the layered structure of $LiMO_2$-based cathode materials (Source: Xu, et al. 2012).

Although NMC cathode materials have high energy density and long cycle life, deteriorations in the structure due to various reasons cause capacity loss and low cycle life. In order to reduce these structural deteriorations, studies are carried out on lithium-rich NMC cathode materials. Lithium-rich NMC cathode materials consist of two phases, Li_2MnO_3 and $LiMO_2$ (M = Ni, Co, Mn) and have a high capacity thanks to their two phases. It has a high energy density due to its high capacity and high nominal voltage, so it is very clear for use in electric vehicles. However, for this, the problem of capacity loss must be largely prevented. Other layered cathode materials used and studied can be listed as Li_2MnO_3, $LiVO_2$, $LiCrO_2$, $LiTiS_2$ (Nitta, et al. 2015).

1. 3. 2 .2. 2. Cathode materials in spinel structure

The most important cathode material with spinel structure (Figure 1.6) is $LiMn_2O_4$. This cathode material has a low specific capacity, but due to its high rated voltage, its specific energy density is close to other cathode materials.

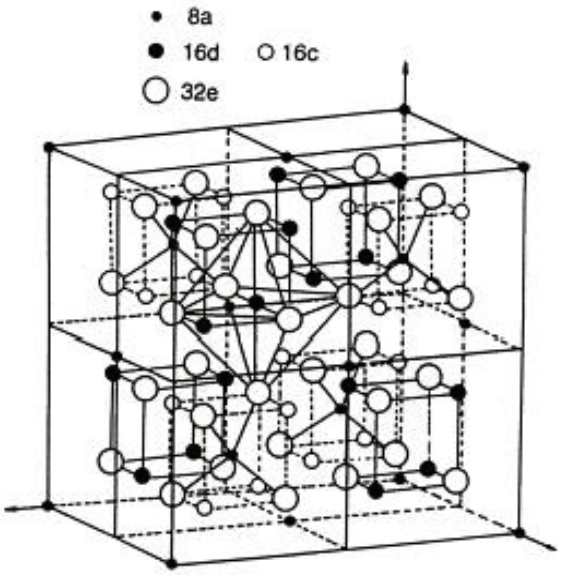

Figure 1.6. The appearance of the spinel structure. (Source: Linden 2002).

$LiNi_{0,5}Mn_{1,5}O_4$, another cathode material with spinel structure, has a higher specific capacity (~147 mAsa/g) than $LiMn_2O_4$ (Hu, et al. 2013). In addition, it is an important advantage that these two materials are low cost and environmentally friendly. However, due to reasons such as the separation of Mn^{+3} from the structure as a result of reactions, the occurrence of Jahn Teller distortion when Mn^{+3} concentration increases and the loss of capacity due to these, studies are being carried out to develop this cathode material (Kang, et al. 2001). While the oxygen atoms in the structure of $LiMn_2O_4$ are similar to the layered structure, unlike the layered structure, ¼ of the Mn atoms in the octahedral position are located in the positions where the lithium atoms are located, leaving ¼ of the octahedral positions empty. That is, the Mn atoms left the 16c position blank. Therefore, the positions adjacent to the Li atoms in the 8a positions remained empty. In this way, the diffusion path of lithium ions became 3-dimensional (8a-16c-8a). For this reason, spinel cathode materials have the highest diffusion rate (Bloom, et al. 2003, Demiray 2007, Hu, et al. 2013, Kang, et al. 2001, Liu, et al. 1996, Xu, et al. 2012).

1. 3. 2. 2. 3. Cathode materials in olivine structure

The most well-known commercial cathode material with olivine structure is $LiFePO_4$. The theoretical capacity of this cathode material is 170 mAsa/g and its nominal voltage is 3.45 V. Although its capacity is higher than other cathode materials, the nominal voltage of this cathode material is also smaller. Although it has high thermal stability and long cycle life without capacitance degradation, its small nominal voltage and low electrical and ionic conductivity prevent it from being widely used. However, it is used in electric and hybrid vehicles, base stations, and storage of energies produced from renewable energy sources (Armand 2004, Chung, et al. 2002, Orendorff and Doughty 2012). In addition, studies are carried out on cathode materials in olivine structure such as $LiMnPO_4$ and $LiCoPO_4$ (Delacourt, et al. 2005, Okada, et al. 2001). The crystal structure of $LiFePO_4$ consists of octahedral FeO_6 and tetrahedral PO_4s. The crystal structure of $LiFePO_4$ in olivine structure is shown in Figure 1.7. These octahedra and tetrahedra contact each other in the b and c plane, but the PO^{4-}tetrahedra do not contact each other (Zhang 2011). In addition, the strong P-O covalent bonds in the orthorhombic olivine crystal structure of $LiFePO_4$ stabilize the Fe^{3+}/Fe^{2+} redox couple, making $LiFePO_4$ stable at high temperatures.

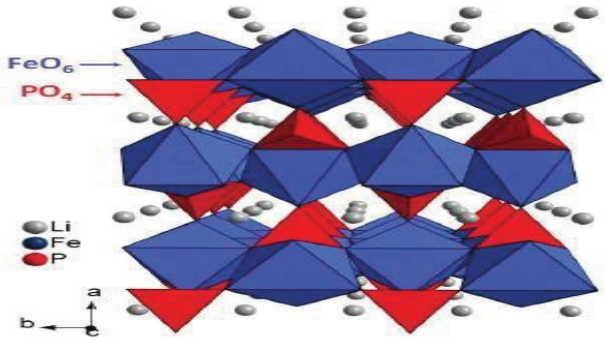

Figure 1.7. Olivine structure of LiMPO4s. (Source: Daniel, et al. 2014).

1. 3. 2. 3. Electrolyte

It is used to provide Li^+ ion transfer between the electrolyte anode and cathode through organic solvents. The electrolyte must not react chemically with lithium and must

be conductive. That is, a good electrolyte must be electrochemically stable and conduct lithium ions very well. Although liquid electrolytes are commonly used today, gel electrolytes and ceramic electrolytes are also used (Linden 2002).

In liquid electrolytes, organic solvents are used to dissolve materials such as LiPF6, $LiBF_4$, $LiN(SO_2CF_2CF_3)_2$, (LiBETI), $LiBC_4O_8$ (LiBOB), $LiPF_3(CF_2CF_3)_3$ (LiFAP) and $LiN(SO_2CF_3)_2$ (LiTFSI). They are used together with carbonates such as ethylene carbonate (EC) and propylene carbonate (PC), diethyl carbonate (DEC) and dimethyl carbonate (DMC) as organic solvents because ethylene carbonate (EC) and propylene carbonate (PC) are solid at room temperature(Denizli 2011) . In general, the electrolytes consist of a mixture of $LiPF_6$ and EC:DMC.

1. 3. 2. 4. Seperator

Separators are placed in lithium ion battery cells to prevent short circuit between anode and cathode and to ensure ion transfer. The separators have a thickness of 10-30 μm, micropores of 0.03–0.1 μm and a pore concentration of 30-50%. Today, polyolefin membranes produced mostly from polyethylene (PE) and polypropylene (PP) are used as separators. In addition to being inexpensive, it is expected from an electrolyte that it has a chemically and mechanically stable structure. In addition, the quality of the separator shows the change of porosity versus temperature. PE loses its porosity at 135°C and PP at 166°C as the melting temperature is reached ("Http://Www.Emc2.Cornell.Edu/Content/View/Battery-Anodes.Html").

1. 3. 3. Working principle of lithium-ion batteries

The working principle of lithium-ion batteries is generally lithium in the cell. It is based on the movement of ions, and in the external circuit, the movement of electrons going in the direction the lithium ions go inside the cell. Working of lithium-ion batteries

In order to understand the principle, charge and discharge mechanisms should be considered separately. A representative representation of the working mechanism of lithium-ion batteries is given in Figure 1.8.

In lithium-ion batteries, during charging, lithium ions are separated from the structure of the cathode material $LiMO_2$ and bonded to the structure of the carbon anode. Meanwhile, electrons move from the cathode to the anode in the external circuit. During discharge, the lithium in the structure of the carbon anode separates and returns to the structure of the cathode. The electron also moves from the external circuit in the same way. In both charge and discharge states, current occurs opposite to the electron direction (Linden 2002).

The reactions taking place are given below; Cathode (Positive electrode) :

In charge state: $LiMO_2 \rightarrow Li1\text{-}xMO_2 + xLi^+ + xe^-$ (2.1)

In the discharge state: $Li1\text{-}xMO_2 + xLi^+ + xe^- \rightarrow LiMO_2$ (2.2) Anode (Negative electrode):

In charge state: $C + xLi^+ + xe\text{-} \rightarrow LixC$ (2.3)

In case of discharge: $LixC \rightarrow C + xLi+ + xe\text{-}$ (2.4) Total reaction:

In charge state: $LiMO2 + C \rightarrow LixC + Li1\text{-}xMO_2$ (2.5)

In case of discharge: $LixC + Li1\text{-}xMO_2 \rightarrow LiMO_2 + C$ (2.6)

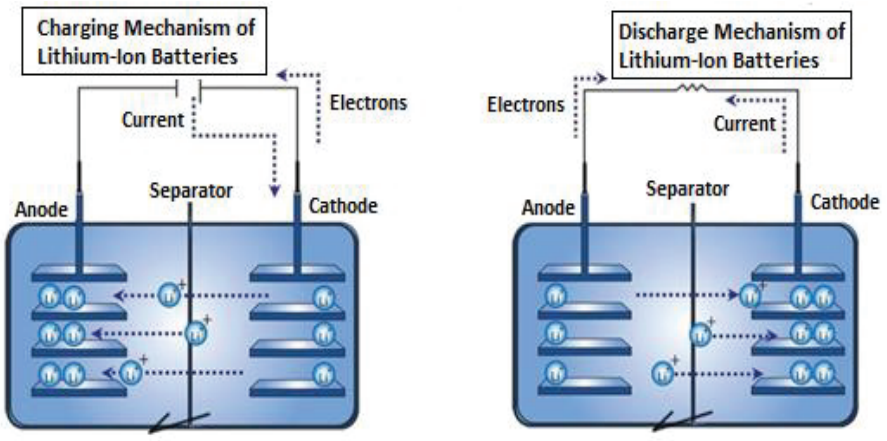

Figure 1.8. Charge and discharge mechanisms of lithium-ion batteries. (Source: Buchmann 2012).

1. 4. NMC and Lithium-rich NMC Cathode Materials

NMC cathode materials have been widely used in lithium-ion batteries in recent years. It has high specific capacity (170 mAsa/g), high nominal voltage (3.8 V), therefore high energy density and long cycle life. Due to these features, it is used in electric vehicles and its use is increasing. In the studies, NMC cathode materials of various compositions are being studied. NMC cathode materials have α-NaFeO2 type layered structure and generally studied NMC compositions LiNi1 / 3Co1 / 3Mn1 / 3O2 (NMC111), $LiNi_{0,5}Co_{0,2}Mn_{0,3}O_2$ (NMC523), $LiNi_{0,8}Co_{0,1}Mn_{0,1}O_2$ (NMC 811).

The results obtained from the studies on these popularly used NMC cathode materials are compared in Table 1.3. Compositions of NMC622, NMC712 and NMC721 are also being studied (Choi and Lee 2016, Pan, et al. 2016)

Table 1.3. First discharge capacities and capacity conservation rates of the most studied NMC cathode materials obtained from experimental studies.

NMC Composition	**First Discharge capacity (ms/g)**	**Capacity Conservation (%)**
NMC111 (Oljaca, et al. 2014)	160 (0,2C)	61 (After 80 cycles with 1C)
NMC523 (Kong, et al. 2014)	201,2 (0,1C)	87.4 (After 60 cycles with 2C)
NMC811 (Lu, et al. 2013)	195,7 (0,1C)	85.2 (at 0.1C after 50 cycles)

NMC cathode materials contain divalent nickel, trivalent cobalt, tetravalent manganese ions. Only Ni and Co undergo redox reactions ($Ni^{2+} \rightarrow Ni^{3+}/Ni^{4+}$; $Co^{3+} \rightarrow Co^{4+}$), while Mn remains tetravalent between 2.5-4.2 V. Therefore, Mn is used to stabilize the structure (Johnson, et al. 2004). The layered NMC structure remains stable when charged above 4.2 V. The reason for this is that when most of the lithium ions in the

structure are separated from the cathode structure during charging, Ni and a small amount of Co enter the tetrahedral lithium positions that lithium discharges and disrupt the structure (Mizushima, et al. 1980). In addition, the increase in oxygen activity on the electrode surface causes oxidation of the electrolyte or oxygen release from the cathode. As a result of these events, problems such as capacity loss and shortening of the cycle life occur (Wang, et al. 2011).

Lithium-rich NMC is a layered cathode material containing Li_2MnO_3 and $LiMO_2$ (M = Ni, Co, Mn) phases. The difference from NMC cathode materials is that it has a Li_2MnO_3 phase. It is possible to represent lithium-rich NMC cathode materials with the formulas $xLi_2MnO_3 \cdot (1-x)LiMO_2$ (M = Ni, Co, Mn) or Li1+x(NiMnCo)1-xO2. Due to the fact that lithium-rich NMC cathode material works at high voltages, offers high capacity, high energy density, low cost and safety, studies are being carried out to make it widely used in electric vehicles. Lithium-rich NMC has an α-NaFeO2 type layered structure. In the structure of NaFeO2, there are Li in Na positions and Ni, Co, Mn in Fe positions. Considering this structure as a modified NaCl structure, tight-packed oxygen atom planes separate the lithium layers from the transition metal-rich layers.

Lithium and transition metals are located in octahedral spaces (Figure 1.9 , Figure 1.10) (Brinkhaus 2015).

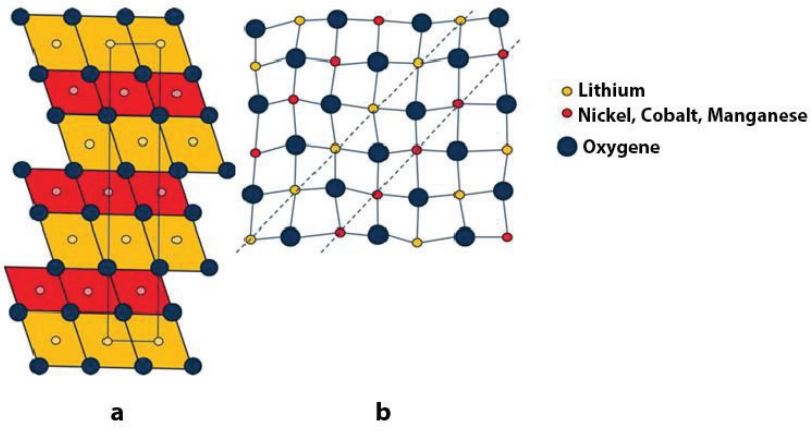

Figure 1.9. a) The 2-dimensional octahedral array in the structure of lithium-rich NMC representation b) the arrangement of atoms. (Source: Brinkhaus 2015).

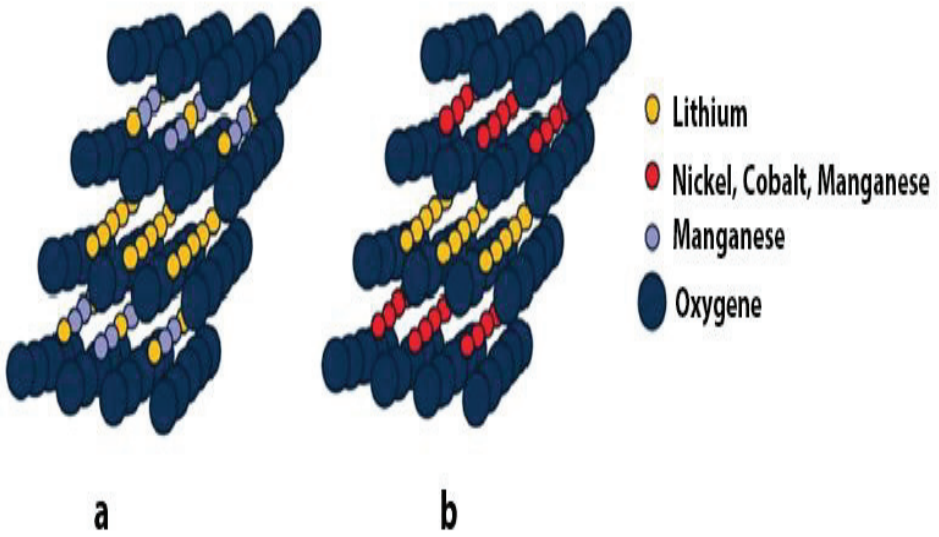

Figure 1.10. a) The 2-dimensional octahedral array in the structure of lithium-rich NMC Representation

b) the arrangement of atoms. (Source: Brinkhaus 2015).

In figure 1.11. in the structure of Li_2MnO_3, while it consists of atoms in the world in a plane between tight planetary facades as phase, manganese remains on the whole surface from the earth to atoms. Coulomb, a block in terms of location between superlattice (Superlattice) and superlattice (Superlattice) in terms of the structure of a block and manganese in a hexagonal shape, and manganese wrapping in the shape of its atoms like a hexagon, as in the example in 3.3, with a honeycomb wrapping. The symmetry of this array is C2/m. It is the observations that 2° health data are found in XRD in studies . That is, $xLi_2MnO_3 \cdot (1 - x)LiMO_2$ is defined as "Li_2MnO_3's symmetry is monoclinic C2/m, while $LiMO_2$'s symmetry is rhombohedral R-3m.z

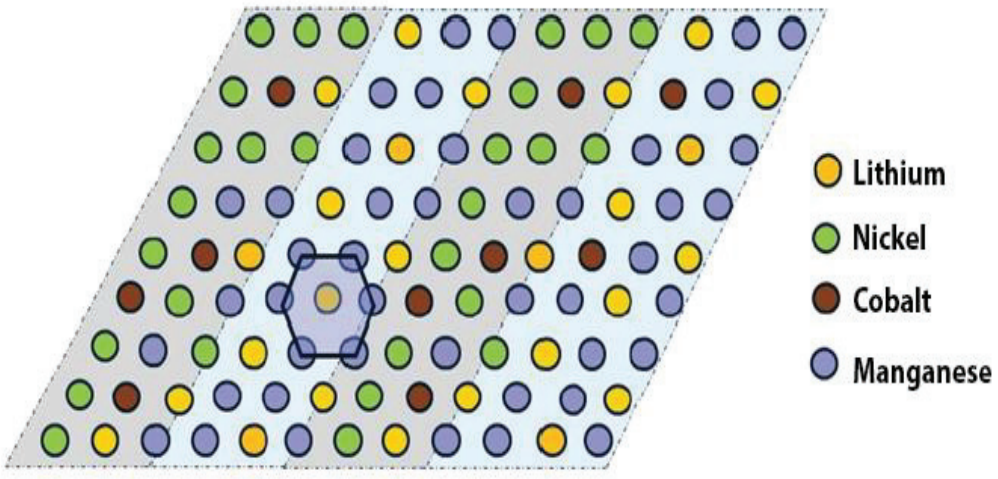

Figure 1.11. Homogeneous distribution of the two phases of lithium-rich NMC s in the transition metal plane, lithium-rich-deficient regions and balpetic (flower) Display of the block in view. (Source: Brinkhaus 2015).

In lithium-ion batteries using lithium-rich NMC cathode material, lithium ions up to 4.4 V are obtained from LiMO2 during initial charging. Divalent nickel (Ni^{2+}) becomes tetravalent (Ni^{4+}) in the range of 3.5-3.9 V, while trivalent cobalt (Ni^{3+}) becomes tetravalent (Ni^{4+}) at 4.4 V. Manganese remains tetravalent (Mn^{4+}). The theoretical capacitance is 130 mAsa/g when all nickel and cobalt are oxidized up to 4.4 V (Yu, et al. 2012). When exceeding 4.3-4.4 V, Li_2O (as Li^+ and O_2) is gained from Li_2MnO_3 up to 5 V. In this way, high capacities are obtained by going to high voltages. Especially the first charge capacity is very high. The first cycle charge is also very important in explaining the structural integrity between Li_2MnO_3 and $LiMO_2$. Ateş et al. explained this phenomenon as the release of oxygen in the first charge and irreversible capacity losses after the first cycle due to the reaction of the electrolyte and the active material (Ates, et al. 2013).

1. 4. 1. Lithium-Rich NMC Production Methods

Lithium-rich NMC cathode materials can be produced by many methods, and the production method affects the purity, particle size and distribution of the produced

material. The most widely used lithium-rich NMC production methods are Pechini method, solid state synthesis, co-precipitation method and sol-gel method.

1. 4. 1. 1. Pechini method

The Pechini method is based on the formation of a polymer matrix as a result of mixing the precursors and pyrolysis of this polymer matrix at high temperature. Polymerization begins when metal salts (or alkoxides) are mixed in a solution of ethylene glycol and citric acid and risen to 100°C. Then, when the pyrolysis temperature is increased, oxidation and pyrolysis take place. As a result of the pyrolysis reaction, the desired material is produced. There is no need to heat the product produced by this method (Kakihana and Yoshimura 1999).

1. 4. 1. 2. Solid state synthesis

Solid state synthesis, which is more difficult to realize than reactions in liquid and gas phases, is based on the logic of exothermic reactions by combining solid precursors at a temperature below their melting temperature. In this method, it is used in metal oxide production because the reactions are at low temperatures and particles with a large surface area are produced. The biggest disadvantage of the solid state synthesis method is that it is difficult to control the stoichiometry of the produced metal oxide (Eker 2006). In this method, processes such as grinding and mixing are applied to the oxides or carbonates, which are the precursors of the material to be produced, to ensure a uniform distribution among the powder particles. Then, if the grinding process is done wet, it is subjected to drying process and then pressed. The pressed samples are sintered at appropriate temperatures and in the appropriate process. There is no need to do any other process on the product resulting from sintering (Arikan 2010).

1. 4. 1. 3. Co-precipitation method

In the co-precipitation method, after the salts of the metals in the material desired to be produced are dissolved in pure water, a basic solution is added and a precipitate is formed at the appropriate pH. The precipitate is formed due to the formation of an insoluble reaction product in the supersaturated solution. The final product is obtained by heat treatment of the precipitate formed. The advantages of this method can be listed as follows (Darab 2010);

1- Low synthesis temperature

2- Low particle size

3- Simplicity of the process

1. 3. 1. 4. Sol-gel method

Sol gel method is one of the most used production methods today due to its advantages such as simplicity, controllability of chemical reactions, requiring less energy, and obtaining submicron sized powders, but it is not preferred commercially due to its long processing time and expensive starting materials. The advantages and disadvantages of the sol-gel method are indicated in Table 1.4.

A colloidal suspension containing solid particles smaller than 500 nm under the influence of Van Der Vaals forces is called sol. If these solid particles start to form three-dimensional solid inorganic network structures in the left as a result of the reactions taking place, gelation begins and when the gelation is completely finished, the resulting structure is called gel. Different processes are applied according to the type of material desired to be produced in the sol-gel method.

Table 1. 4. The advantages and disadvantages of the sol-gel method

Advantage	Disadvantage
Having a simple method	The process takes a long time
Chemical reactions can be controlled	Expensive starting materials
Obtaining high purity and submicron size powder	Remaining carbon and hydroxyl in the structure
Does not require much energy	Loss of material
Application at low temperatures	Being sensitive to moisture
Suitable for surface modification and doping	Difficult to produce on large scales
Ability to produce products in desired composition	

Salts (acetate, nitrate, etc.) or alkoxides of the components of the material desired to be produced in the sol-gel method are dissolved in a suitable solvent (pure water or alcohol) and then a chelating agent is added. After the solution reaches the required pH and temperature, sol is formed and then gelation begins. After the gelation takes place, the desired material is obtained after the processes depending on the product type such as extrusion, drying, and heat treatment are applied to the gel formed.

It is possible to list the main steps of the sol-gel method as follows;

1. Hydrolysis

2. Condensation

3. Polymerization

4. Gelling

The first reactions that take place in solution are hydrolysis reactions. At this stage, OR groups are transformed into OH groups by hydrolysis reaction. Parameters such as pH, temperature, amount of water, catalyst type, solvent concentration affect hydrolysis reactions

The hydrolysis reaction takes place as follows;

$$M(OR)n + H_2O \leftrightarrow HO\text{-}M(OR)n\text{-}1 + R\text{-}OH \quad (3.1)$$

The reaction and combination of two materials, which are the products of hydrolysis, with each other is called condensation reaction. This reaction is as follows;

$(OR)3M\text{-}OH + HO\text{-}M(OR)3 \rightarrow (OR)3M\text{-}O\text{-}M(OR)3 + H_2O$ (3.2) These monomers formed as a result of condensation reactions turn into particles as a result of polymerization and these particles grow. The enlarged particles start to gel by forming a network structure between each other and then a gel is formed. After drying the formed gel and applying heat treatment, the desired product is obtained ("Http://Www.Lehigh.Edu/Imi/Teched/Lecbasic/Marques_Sol_Gel.Pdf"). There are many parameters such as composition, amount of chelating agent, pH and temperature that affect the formation of these stages.

1. 4. 2. Lithium-Rich NMC Film Production Methods

Lithium-rich NMC powders are generally coated on metal substrates. Applicable coating methods;

• Spin coating

• Dipped coating

• Lamination

• Laminar coating

• Spray coating

• Roller coating

• Print coating

Among these coating methods, the most used methods for coating lithium-rich NMC are spin coating, dip coating and lamination.

1. 4. 2. 1. Spin coating

The spin coating method is to drop the coating material on the center of the substrate to be coated and rotate it at the required rotation speed to the surface.

distribution is based on (Figure 1.12). After the solution spreads on the surface, the coating process is applied by evaporation of the solvent.

After the dripping process, the substrate is accelerated until it reaches the required rotational speed, and thanks to the centrifugal force, the coating solution is distributed on the surface and the excess solution is removed from the surface.

The distribution of the coating material on the surface can be done statically or dynamically. In static dispensing, rotation is performed after dripping, while in dynamic distribution, dripping is performed while the pad is rotating. The thickness of the coating depends on parameters such as viscosity, spin speed, spin time as well as the evaporation process. As the rotation speed and time increases, the coating thickness decreases (Rehg and Higgins 1992).

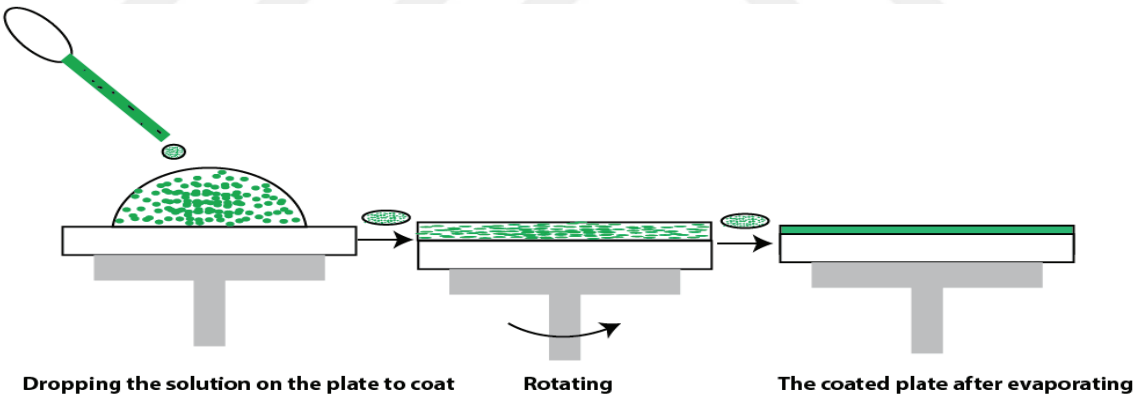

Figure 1.12. Illustration of the spin coating method .
(Source:"Http://Www.Sneresearch.Com/Eng/Info/Show.Php?C_Id=4970&Pg=5&S_Sor t=&Sub_Ca T=&S_Type=&S_Word= ").

1. 4. 2. 2. Dipped coating

The dip coating method (Figure 1.13) is one of the most known methods for making thin film coating on the substrate surface. The most important advantages of this method are that the process is simple, that it can be applied in series and that it can be re-coated on the coating. The disadvantages are that when a surface is to be coated, a mask is used on the other surface and problems are experienced in adhering to the surface. The gravitational force, friction force between the solution and the substrate surface and surface tension affect the surface adhesion problem, which is one of the biggest problems of this method.

The dip coating method has a simple logic, such as coating the substrate by dipping it into the solution of the material to be coated. To explain in more detail, the substrate is immersed in the solution of the desired material and kept in the solution for the required time. After the time that the litter material has to stay in the solution is over, it is removed at a constant speed in order to prevent the heterogeneity that will occur when it is removed with acceleration. The rate at which the substrate is removed from the solution also affects the coating thickness. The desired film is obtained by evaporating the solvents in the coated substrate (Brinker, et al. 1991).

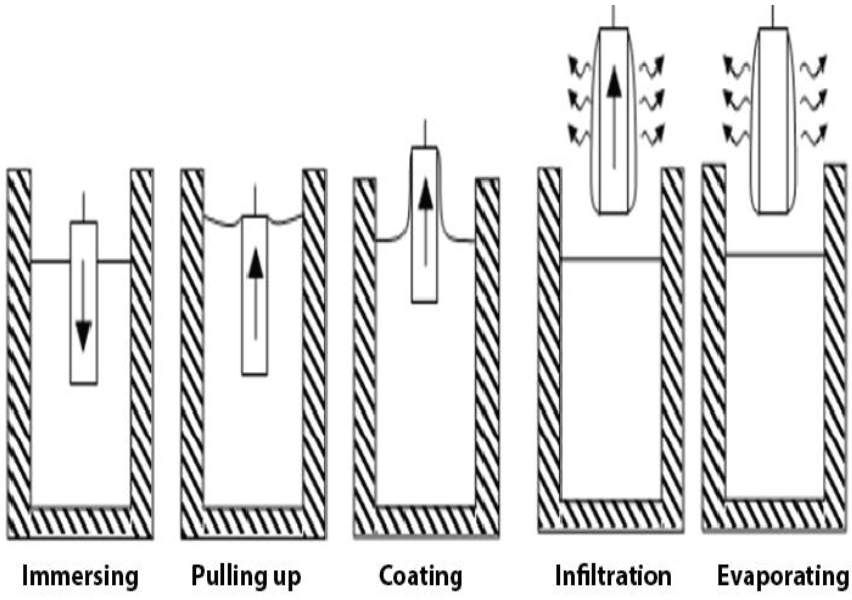

Figure 1.13. The main stages of the dip coating method.(Source: Brinker, et al. 1991)

1. 4. 2. 3. Lamination

The lamination method is based on the principle of applying the material to be coated on the substrate surface with the help of a special knife (Doctor blade) shown in Figure 1.14 and drying it in the device shown in Figure 1.15. The biggest advantage of the lamination method is that it is a simple and inexpensive method. In addition to its advantages such as uniform coating and mass production, it also has a disadvantage such as fluctuation on the coated surface.

To explain the lamination process in detail; After the pad material is cleaned, it is fixed to the lamination device. Then, the mixture consisting of powder, binder and solvent of the material to be coated is dripped onto the part of the substrate closest to the blade. The blade (Doctor blade) drives the mixture onto the substrate surface at the desired speed and at the desired thickness. Solvent after this process evaporated and the substrate is coated. In the lamination method, the thickness is adjusted by raising and lowering the blade, so coating can be made at certain thicknesses. Although the coating ranges that can be made vary according to the blade used, they are generally between 10-1000 μm. In thinner coatings, even small unevenness on the lower surface can cause the underlay to deform. Apart from the height of the blade, other factors affecting the quality of the films produced by the lamination method are the viscosity of the mixture, temperature, speed of the blade, particle size of the powder used, the roughness of the substrate surface and the humidity of the substrate surface (Bierwagen 1992).

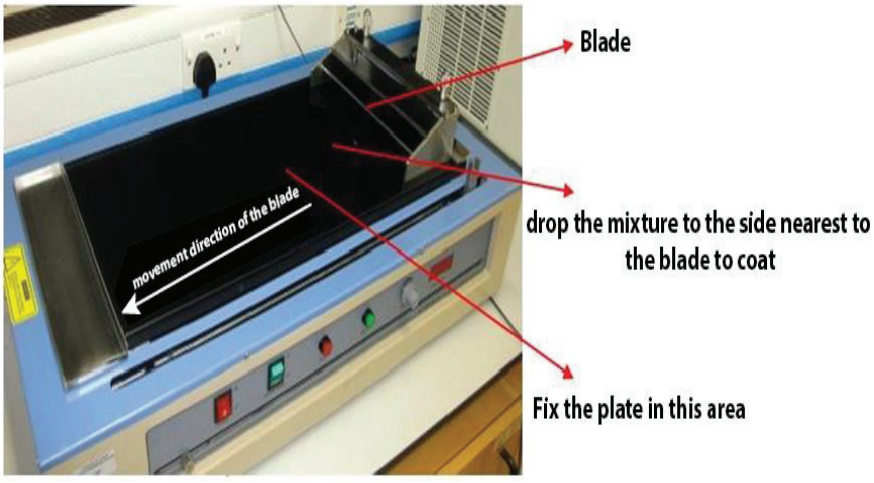

Figure 1.14. Laminating device

Figure 1.15. The blade used in the laminator (Doctor Blade). (Source: "Http://Www.Mtixtl.Com/Micrometeradjustablefilmapplicator-250mmeq-Se-Ktq-250.Aspx").

1. 4. 3. Problems and Solutions of Lithium-Rich NMC Cathode Materials

Studies on lithium-rich NMC cathode materials continue with intense efforts of researchers. The most effort of the researchers is on the solutions of the problems of lithium-rich NMC cathode materials. In order to work on the solutions of the problems of lithium-rich NMC cathode materials, it is necessary to understand their problems first.

These problems can be listed as follows (Wohlfahrt-Mehrens, et al. 2004);

• Structural changes occur during cycles
• Electrolyte oxidation and irreversible loss of Li
• Dissolution / loss of metal ions in the structure

The structures of the layered lithium-rich NMC cathode materials can transform from layered to spinel during cycles. The reason for this is that during the exit of Li ions from the cathode, Mn atoms quickly fill the tetrahedral spaces in the Li plane, however, Li atoms are settled in the tetrahedral spaces on the other side of the octahedral space emptied from the Mn atoms (Reed, et al. 2001). The transformation of the structure from layered to spinel due to these atom migrations prevents lithium inflows and outflows. Blocking Li inlets and outlets negatively affects speed performance and long cycles. To solve this problem, alkali metal additives such as Na, K, Mg are generally used. In the studies, it was stated that alkali metals do not leave the octahedral spaces and do not go

to the tetrahedral spaces, which makes the transformation of the structure from layered to spinel difficult (He, et al. 2013, Jin, et al. 2014, Li, et al. 2014).

Oxygen loss from the cathode and subsequent oxidation of the electrolyte is another problem experienced in lithium-rich NMC cathode materials. This problem is experienced after the Li_2MnO_3 phase is activated when the voltage rises above 4.4 V during the first charge. As a result of the release of Li_2O from the activated Li_2MnO_3 to the electrolyte, it caused both the inability of Li to return to the cathode and the formation of an oxide layer between the cathode and the electrolyte by reacting with the oxygen passing into the electrolyte. As a result of these events, especially after the first charge capacity due to irreversible loss of Li, great decreases are observed, as well as the oxidation of the electrolyte by the oxygen passing into the electrolyte and the formation of an oxide layer at the cathode-electrolyte interface, resulting in capacity losses and decreases in speed performance in the ongoing cycles (Zhou, et al. 2016).

Another problem for which studies have been made is the separation of metal ions from the structure by HF attacks. The moisture remaining in the electrolyte reacts with the electrolyte and turns into HF, while HF reacts with the cathode and removes the metal ions in the structure. This problem is particularly
It shows its effect from the second cycle and causes capacity losses.
The reactions that take place during this problem are as follows(Andersson, et al. 2002);
$LiPF_6 + 4H_2O \rightarrow 5HF + LiF + H_3PO_4$ (3.1) $LiMO_2 + 2xHF \rightarrow 2xLiF + Li(1-2x)MO(2-x) + xH_2O$ (3.2)

These reactions, which take place, cause loss of capacity by removing metal ions from the structure. In order to solve this problem, besides the studies to develop different electrolytes, studies are mainly carried out on the application of metal oxide coatings. Metal oxide surface modification applications such as Al_2O_3, ZrO_2, SnO_2, ZnO, MnO_2, Sm_2O_3, V_2O_5 are applied not only to solve this problem, but also to solve other problems mentioned before or to minimize the effects of the problems (He, et al. 2016, Jin, et al. 2016, Kong, et al. 2016, Li, et al. 2016, Shi, et al. 2013, Wu and Manthiram 2009, Zhou, et al. 2016).

1. 4. 3. 1. Metal oxide surface modification

Rapid capacity losses, which are the reason why lithium-rich NMC cathode materials have not been commercialized yet, should be prevented. For this purpose, metal

oxide surface modifications are made to the cathode materials. Table 1.5. shows the results obtained from some metal oxide surface modifications applied to lithium-rich NMC cathode materials in the literature.

Kong et al. made thin film ZrO_2 coating by ALD method. In their study, they aimed to prevent the increase in capacity loss with increasing temperature. At the end of this study, they stated that the surface modification they made prevented the loss of metal ions as a result of HF attacks and increased the capacity conservation at both 25°C and 55°C by stabilizing the surface structure(Kong, et al. 2016).

Jin et al. applied MnO_2 surface modification by sol-gel method and explained that their surface modification reduced the irreversible capacity loss after the first charge. They stated that the reason for this was that the separation of Li_2O from the layered structure was prevented by the MnO_2 surface modification. They also mentioned that MnO_2 surface modification increases Li^+ diffusion (Jin, et al. 2016).

Table 1.5 Comparison of electrochemical performances of different surface modifications applied to lithium-rich NMC cathode materials.

Article Name	**Coating Made**	**Applied Method**	**Electrochemical Performance**
La_2O_3-coated $Li_{1.2}Mn_{0.54}Ni_{0.13}Co_{0.13}O_2$ as cathode materials with enhanced specific capacity and cycling stability for lithium-ion batteries (Zhou, et al. 2016).	La_2O_3	Sol gel method	Capacity retention rate of 71% after 100 cycles, discharge capacity of 201.4 mA/g
The role of SnO_2 surface coating in the electrochemical performance of $Li_{1.2}Mn_{0.54}Co_{0.13}Ni_{0.13}O_2$ cathode materials (Li, et al. 2016).	SnO_2	liquid phase method	Capacity retention rate of 86.8% after 150 cycles, 214 mAs/g discharge capacity

(Cont. on next page)

Table 1.5 (Cont.)

Effect of Sm_2O_3 modification on $Li[Li_{0.2}Mn_{0.56}Ni_{0.16}Co_{0.08}]O_2$ cathode material for lithium ion batteries(Shi, et al. 2013).	Sm_2O_3	Sol gel method	91.5% capacity retention rate at the end of 80 cycles, 214 mAh / g discharge capacity
Effects of amorphous V_2O_5 coating on the electrochemical properties of $Li[Li_{0.2}Mn_{0.54}Ni_{0.13}Co_{0.13}]O_2$ as cathode material for Li-ion batteries (He, et al. 2016).	V_2O_5	Sol gel method	80.2% capacity retention rate after 50 cycles, 202.2 mAs/g discharge capacity

1. 4. 3. 2. Surface modification with Aluminum

Besides the previously mentioned surface modification materials, Al_2O_3 is also used for surface modification. Metal oxide surface modifications positively affect the two most important problems of lithium-rich NMC cathode materials. Al_2O_3 surface modification likewise suppresses the loss of metal ions from the cathode as a result of HF attacks and the negative effects of Li_2O released into the electrolyte by the decomposition of Li_2MnO_3, which is activated after 4.4 V in the first charge. The negative effects of Li_2O formation are that it causes Li atoms to remain in the electrolyte irreversibly and to oxidize the electrolyte. All these negativities cause capacity losses. It is known that Al_2O_3 not only reduces the capacity losses arising from these problems, but also increases the structural stability (Zhou, et al. 2016). From this point of view, Al_2O_3 surface modification stands out among metal oxide surface modifications.

Wu and Manthiram applied popular metal oxide surface modifications such as 3% by weight Al_2O_3, $AlPO_4$, ZrO_2, ZnO, CeO_2 and SiO_2 to the lithium-rich NMC cathode material and compared the results obtained from these surface modifications. In contrast to the 254 mAsa/g initial discharge capacity of the sample without surface modification at 0.05C, the Al_2O_3, $AlPO_4$, ZrO_2 and ZnO surface modifications are 284, 260, 251,252 mA/g, respectively. They gave a first discharge capacity of 259, 261 mAsa/g. Considering

the discharge capacity conservations at the end of 30 cycles, Al_2O_3, $AlPO_4$, ZrO_2 and ZnO surface modifications obtained results such as 92%, 81%, 83% and 87%, respectively, while the sample without surface modification had a capacity conservation of 89%.

While the initial charge capacity of the sample without surface modification was 334 mAsa/g, the initial discharge capacity was found to be 254 mAsa/g. The initial charge and discharge capacities of the Al_2O_3 surface modified sample are 326 mAs/g and 285 mAs/g, respectively. Similar results were obtained with the Al_2O_3 coated sample in other metal oxide coatings. In their study, Wu and Manthiram based the metal oxide modifications, especially the Al_2O_3 surface modification sample, to have high discharge capacities and discharge capacity conservations, on the prevention of oxygen ion loss in the cathode structure by these surface modifications (Wu and Manthiram 2009). As mentioned before, the loss of oxygen ions occurs when Li_2O is released from Li_2MnO_3 to the electrolyte when high voltage is reached in the first charge. The big difference between the first charge and first discharge capacities of the sample without surface modification is also an indication of this. As seen in this study, the difference between the initial charge and first discharge capacities is much smaller in the Al_2O_3 modified sample than in the unmodified sample. This shows that the Al_2O_3 surface modification prevents Li_2O release to the electrolyte. Having high initial discharge capacity compared to other metal oxide surface modifications as well as having high capacity conservation as a result of increasing cycles shows that Al_2O_3 surface modification is superior to other surface modifications.

In another study by Zhao et al., 1.5 wt% Al_2O_3 surface modification was applied to the lithium-rich NMC cathode material and tested at a speed of 0.2C. As a result of this study, the first charge capacity of the sample without surface modification was 340 mAsa/g and the first discharge capacity was 270 mAsa/g, while the first charge capacity of the sample with surface modification was 326 mAsa/g and the first discharge capacity was 285 mAsa/g. After 30 cycles, approximately, the discharge capacity conservations of the unmodified and Al_2O_3 surface modified samples were 79% and 85%, respectively, while they were 70% and 79% after 50 cycles. In their study, they explained that the sample with Al_2O_3 surface modification had higher capacity conservation than the other sample, with the Al_2O_3 surface modification preventing the loss of metal ions with HF attacks and the deterioration of the structural stability on the surface (Zhou, et al. 2016).

Looking at the results of the study by Zhao et al., it seems that these results are better than the results of the study by Wu and Manthiram. The fact that Zhao et al.'s sample with 1.5% wt Al_2O_3 surface modification had the same charge and discharge capacities as the 3% wt% Al_2O_3 surface modification sample in the other study, especially that it achieved this at a C speed 4 times higher than the other 1.5% Al_2O_3 surface modification. made the modified sample superior. Although a very accurate comparison cannot be made because of the different C velocities after 30 cycles, the sample with 1.5% wt Al_2O_3 surface modification is considered to be a more successful surface modification since it provides a 6% improvement when compared to its own surface modification samples.

In this study, it is aimed to improve the electrochemical performance without sacrificing high capacity conservation, thanks to a surface modification with less AlOOH percentage (0.5%) by weight, therefore lower internal resistance and less cost. In line with this aim, it is aimed to produce Al coated NMC cathode material with 0.5% AlOOH surface modification without surface modification by co-precipitation method and to examine its electrochemical performances.

CHAPTER 2

EXPERIMENTAL

2. 1. Experimental Introduction

In this thesis, detailed information about the materials used in the experiments, the conditions in which these experiments were carried out, their construction and applied characterizations will be given under the main heading of experimental studies. The flow chart of the study is shown in Figure . The main stages of this flow chart are divided as $Ni_{0.6}Co_{0.2}Mn_{0.2}O_2$ powder production, AlOOH surface coating, cathode film production, electrochemical tests and characterizations.

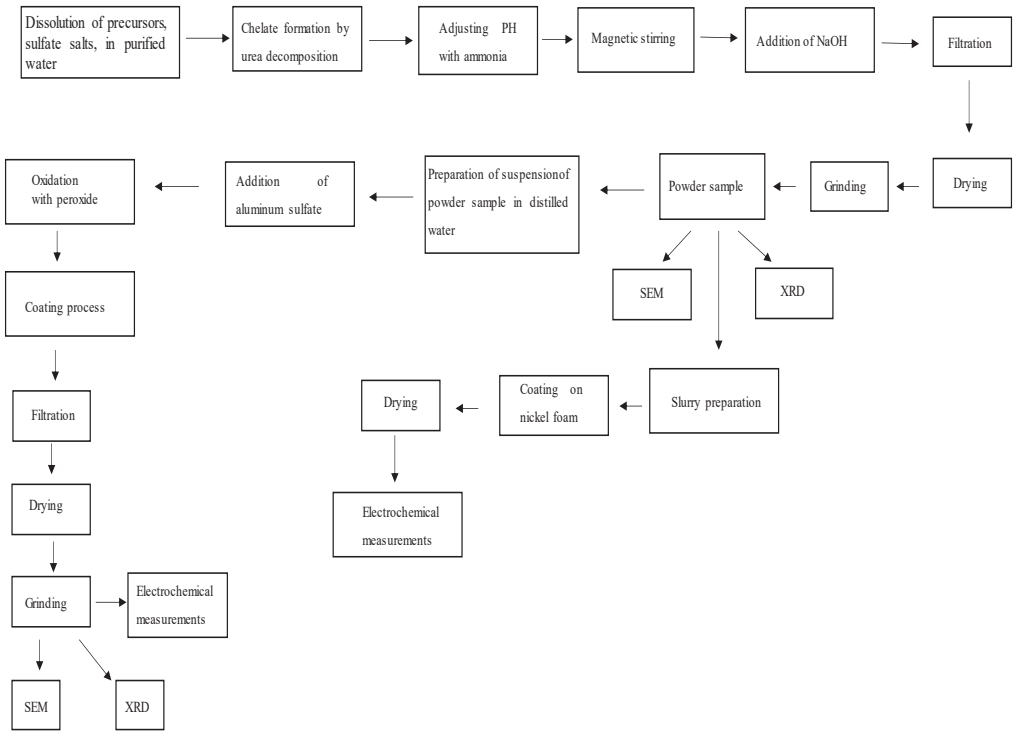

Figure 2.1. Experimental Procedure

2. 2. Synthesis of Hierarchical Nanoporous Ni(OH)2.

Hierarchical nickel hydroxide is synthesized by the redeposition self-template method. In the first step of the procedure, 0.1mol of nickel nitrate and 0.25mol of urea are dissolved in 20 ml of distilled water. This solution is left to stir with the aid of a magnetic stirrer at room temperature for 30 minutes. After 30 minutes, it is observed that the solution turns green. This solution is then taken and transferred to a 3-necked balloon jug. In this environment, it is left to stir for 6 hours at 95 degrees. As a result of the mixing operation, it is observed that the color of the solution turns blue. After this stage, naoh solution is added to the solution at a rate of 40 ml per hour and the mixing process continues at a constant temperature of 95 degrees. After approximately 2.5 hours, the color of the solution turns transparent and the base addition process is finished. The resulting solution is collected by centrifugation and washed with ethanol and deionized water. It is then left to dry at 50 degrees Celsius.

2. 3. Synthesis of co-mn doped $Ni(OH)_2$

In the second step of the procedure, 0.06mol of nickel nitrate and 0.25mol of urea are dissolved in 20 ml of distilled water. This solution is left to stir with the aid of a magnetic stirrer at room temperature for 30 minutes. After 30 minutes, it is observed that the solution turns green. This solution is then taken and transferred to a 3-necked balloon jug. In this environment, it is left to stir for 6 hours at 95 degrees. As a result of the mixing operation, it is observed that the color of the solution turns blue. After observing that the color turns blue, 0.02 moles of manganese nitrate and 0.02 moles of cobalt nitrate are added into the solution, after stirring for a short time, sodium hydroxide solution is added at a rate of 40 ml per hour and the reaction continues at 95 degrees. The reaction is terminated when the color turns colorless. The product obtained is washed with deionized water and ethanol and left to dry at 50 degrees. The entire procedure takes approximately 9.5 hours and takes much less time than procedures such as the reprecipitation and hydrothermal method.

2. 4. Modification of the surface with aluminum

In the 3rd step, it is aimed to modify the surface of the nickel hydroxide structure obtained in the 2nd step with aluminum. First, the nickel hydroxide structure obtained in the 2nd step is added into 50 ml of water and a suspension is formed. 0.1025 grams of aluminum nitrate is added to the resulting suspension and left to dissolve at 60 degrees. No color change is observed. To the solution formed after a mixing period of 30 minutes; A total of 100 ml of naoh and a total of 25 ml of peroxide solution are added. The insertion process takes 30 minutes. After the addition is complete, the reaction is left to stir for 12 hours. After 12 hours, the reaction ends. It is seen that the color of the solution darkens due to peroxide. After the solution obtained is washed with the help of distilled water by filtration method, calcination method is applied and the obtained material is ready for analysis.

2. 5. Cathode production stage

At this stage, the electrode will be made and applied. First of all, to prepare the electrode, polyvinyl alcohol (PVA) and polyvinyl prolidon (PVP) will be dissolved in hot water to form a binder (glue) solution. Then, the glue obtained by mixing nickel hydroxide and carbon black will be made into paste with the solution and the nickel foam will be spread on it and fed, and after drying in room temperature, it will be kept in an oven at 85-95°C for 9-11 hours. After the drying phase, the electrode will be made ready by keeping it under 1-3 MPa (mega pascal) pressure for 1-2 hours.

Figure 2.2. Example of binder (glue) for nickel hydroxide

Figure 2.3.Empty nickel electrodes

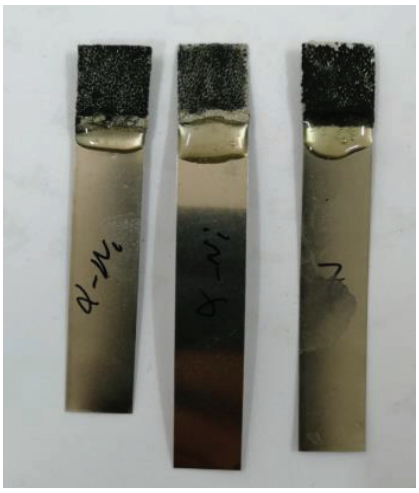

Figure 2.4. Electrodes with alpha-$Ni(OH)_2$ and beta-$Ni(OH)_2$ charges

2. 6. Methods of Characterization

In this study, in addition to material characterization methods such as XRD and SEM, electrochemical characterization methods such as cyclic voltammetry test and chronoamperometry were applied to measure the electrochemical performance of the produced cathode materials.

2. 6. 1. Tap density measurements

Tap density measurements were made with the Tap Dense-TD 101 device. The ASTM method was used. 300 taps per minute were performed and tap density was determined.

2. 6. 2. XRD measurements

It is an analytical technique that gives information about various crystal forms or phases in the structures of solid and powder samples. This technique gives information

about the phases contained in the material and the concentration of these phases, the amount of non-crystalline phases and the crystal size.

The device used in Xrd measurements is Philips X'Pert Pro. With the help of measurements, the crystal structure of the product was determined. Scanned between 5-90 θ.

2. 6. 3. Sem measurements

It can display the structures of materials in micro and nano dimensions. The SE detector provides a topographic 3-dimensional image, and the BSE detector provides a 2-dimensional image based on atomic contrast. In addition, with the EDX detector, the elemental content of the structures can be found quantitatively and qualitatively, and the distribution of elements on the picture can be monitored by mapping. FEI QUANTA 250 FEG device was used during sem measurements. Surface morphology was investigated. Chemical composition was determined in EDX.

2. 6. 4. Electrochemical tests

Cyclic voltammetry analyzes were performed with Metroohm Autolab PGSTAT 204 model galvanostat/potentiostat at scanning rates of 0.01 mV/sec and at room temperature. All cyclic voltammetry data were recorded for 100 cycles. Chronoamperometric analyzes were performed at 0.8 V to measure the maximum current value as the time changes. All chronamperometric measurements were performed for 5h.

CHAPTER 3

RESULT AND DISCUSSION

3. 1. The growth process of $Ni_{0.6}Mn_{0.2}Co_{0.2}(OH)_2$

The detailed formation process of $Ni_{0.6}Mn_{0.2}Co_{0.2}(OH)_2$ contains two stages: Synthesis of the Template-$Ni(OH)_2$ and regrowth by NaOH deposition. During the first stage, hierarchical porous Template-$Ni(OH)_2$ was produced by urea hydrolysis. This process continues until the reaction reaches equilibrium (about 6 h), when the yield of Template-$Ni(OH)_2$ did not increase with extending the reaction time. In this stage two main factors of obtaining high specific surface area $Ni_{0.6}Mn_{0.2}Co_{0.2}(OH)_2$ were achieved: first, Template-$Ni(OH)_2$ was formed in the reactant solution; second, NH_3 coming from the hydrolysis of urea was released as in the equation: $CO(NH_2)_2 + H_2O \rightarrow CO_2 + 2NH_3$ which will form the $[Ni(NH_3)_x^{2+}]$ complexes with the residual Ni^{2+} species in the solution and reaches saturation. In the second stage, as prepared hierarchical porous Template-$Ni(OH)_2$ acted as a template and NaOH acted as a precipitating agent (the third key factor for obtaining high specific surface area $Ni_{0.6}Mn_{0.2}Co_{0.2}(OH)_2$). The equilibrium of the saturated solution was quickly broken by dropping the NaOH solution and new precipitate phase formed. The new precipitate phase was combined with a large number of nucleation sites provided by hierarchical Template-$Ni(OH)_2$, which are favorable for the nucleation and the formation of ultrathin $Ni(OH)_2$ platelets along the surface of hierarchical Template-$Ni(OH)_2$. For improving the conductivity of $Ni(OH)_2$, we synthesized $Ni_{0.6}Mn_{0.2}Co_{0.2}(OH)_2$ by adding Co^{2+} and Mn^{2+} in the second-stage process.

3. 2. Sem images

The detailed morphology of Al-coated $Ni_{0.6}Mn_{0.2}Co_{0.2}(OH)_2$, commercial $Ni(OH)_2$ and as-prepared $Ni_{0.6}Mn_{0.2}Co_{0.2}(OH)_2$ were characterized by scanning electron microscopy (SEM). We can see that $Ni(OH)_2$ (~10 μm) and $Ni_{0.6}Mn_{0.2}Co_{0.2}(OH)_2$ (<10 μm) display a similar uniform spherical morphology with a diameter of about 10 μm. The average size of Al-coated $Ni_{0.6}Mn_{0.2}Co_{0.2}(OH)_2$ (~20 μm) is larger than that of the $Ni_{0.6}Mn_{0.2}Co_{0.2}(OH)_2$, which is due to the AlOOH deposition along the surface of

hierarchical $Ni_{0.6}Mn_{0.2}Co_{0.2}(OH)_2$ in the coating process. Besides, Al-coated $Ni_{0.6}Mn_{0.2}Co_{0.2}(OH)_2$ has relatively poor uniformity in particle size and contain two morphological structures: relatively uniform spherical particles and some small fragments. These small fragments may stem from the breaking of some unstable structures under intense agitation. Magnified images of the microspheres show that all the products exhibit hierarchical porous structures, and the pore radius after NaOH redeposition is substantially larger than before.

Figure 3.1. Sem image of commercial product

For the commercial product;it was observed that the particle size was uniformly distributed at 10 micrometer reduction. Particle sizes are homogeneously distributed. It is understood that the spherical structure has been fully reached. Spherical structure is the desired structure for nmc cathodes. The spherical structure ensures that the cathode material is properly stacked on the collector.

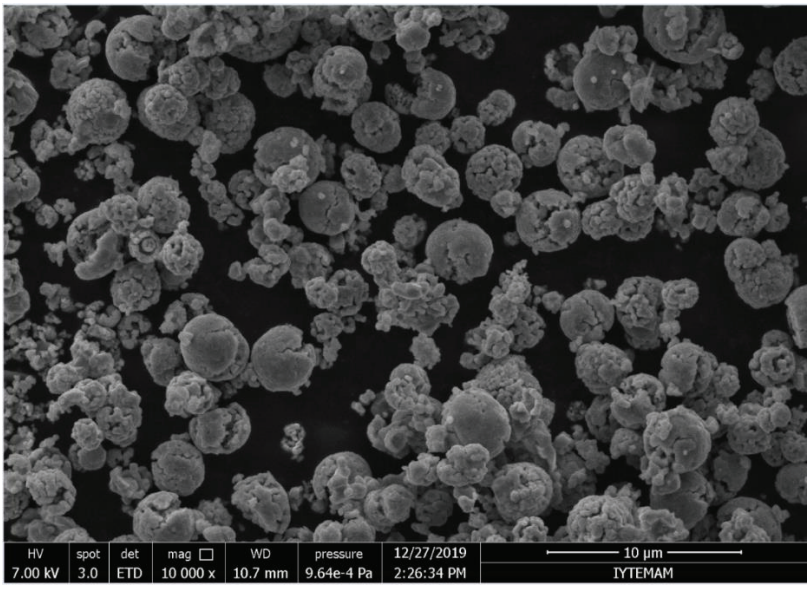

Figure 3.2. Sem image of $Ni_{0.6}Mn_{0.2}Co_{0.2}(OH)_2$

For the $Ni_{0.6}Mn_{0.2}Co_{0.2}(OH)_2$,it was observed that the spherical structure was reached at 10 micrometer reduction. It is observed that the spherical structure is slightly distorted during Nmc synthesis. It has also been observed that there are small and non-round particles in between. It can be said that the structure is uniform. Crystal structure has been reached.

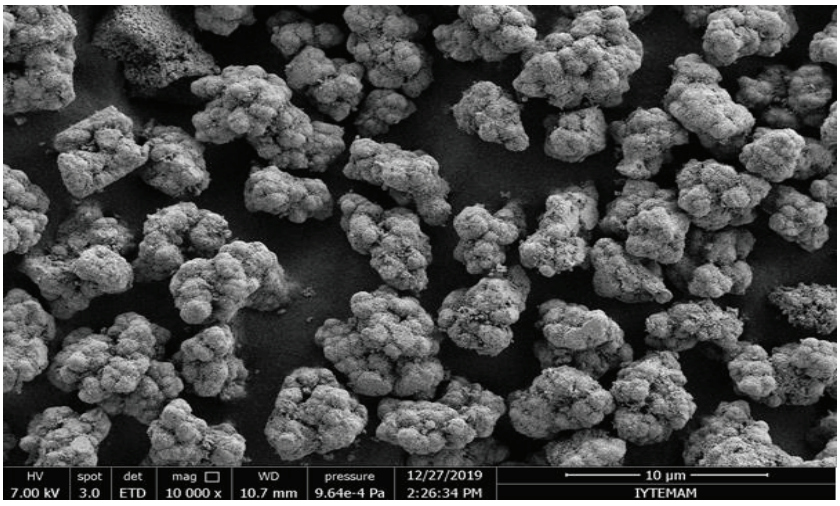

Figure 3.3. Sem image of Al coated $Ni_{0.6}Mn_{0.2}Co_{0.2}(OH)_2$

For the Al coated $Ni_{0.6}Mn_{0.2}Co_{0.2}(OH)_2$, at 10 micrometer reduction, it was observed that the spherical structure deteriorated after aluminum coating. Particles are aggregated by bonding to each other. It was observed that the size of each cluster was

close to each other. Although the crystal structure is slightly distorted during synthesis, the structure is still uniform and ready for electrochemical analysis.

3. 3. XRD Patterns

X-ray diffraction (XRD) patterns of the as-fabricated samples and commercial β-$Ni(OH)_2$. The peaks of commercial $Ni(OH)_2$ appeared at 2θ = 12.3°, 24.7, 33.2°, and 59.2°, corresponding to the (003), (006), (101), and (110) diffraction planes of α-$Ni(OH)_2$, in agreement with many previous reports. The peaks of Al-coated Ni0.6Mn0.2Co0.2(OH)2 and $Ni_{0.6}Mn_{0.2}Co_{0.2}(OH)_2$ can be indexed to α-phase nickel hydroxide, which is because the α-type $Ni(OH)_2$ (Template-$Ni(OH)_2$) is unstable in strong alkaline media and may transform to β-$Ni(OH)_2$. Because Ni and Co are neighboring elements in the Periodic Table, which have similar physical and chemical properties, the XRD pattern of $Ni_{0.6}Mn_{0.2}Co_{0.2}(OH)_2$ is similar to $Ni(OH)_2$. Compared with Commercial-$Ni(OH)_2$, $Ni(OH)_2$ and $Ni_{0.6}Mn_{0.2}Co_{0.2}(OH)_2$ samples show broadening of the reflection peaks, which can be attributed to poor crystallinity and a large number of defects. And the shoulder peak near 2θ = 12° shows that both $Ni(OH)_2$ and $Ni_{0.6}Mn_{0.2}Co_{0.2}(OH)_2$ still have residual α-phases. The low crystallinity observed can mainly be attributed to the fast kinetics of the $Ni(OH)_2$ formation and continuously vigorous stirring during synthesis.

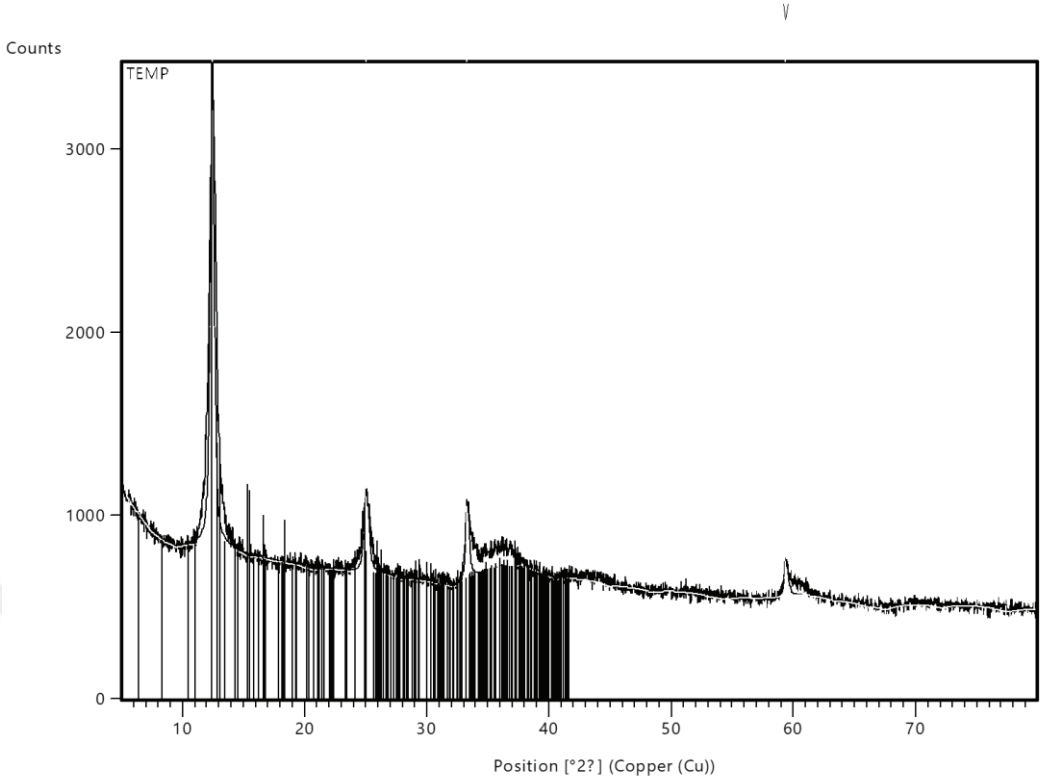

Figure 3.4. Xrd result of commercial product

X-ray diffraction (XRD) patterns of the as-fabricated samples and commercial β-$Ni(OH)_2$. The peaks of commercial $Ni(OH)_2$ appeared at 2θ = 12.3°, 24.7, 33.2°, and 59.2°, corresponding to the (003), (006), (101), and (110) diffraction planes of α-$Ni(OH)_2$, in agreement with many previous reports.

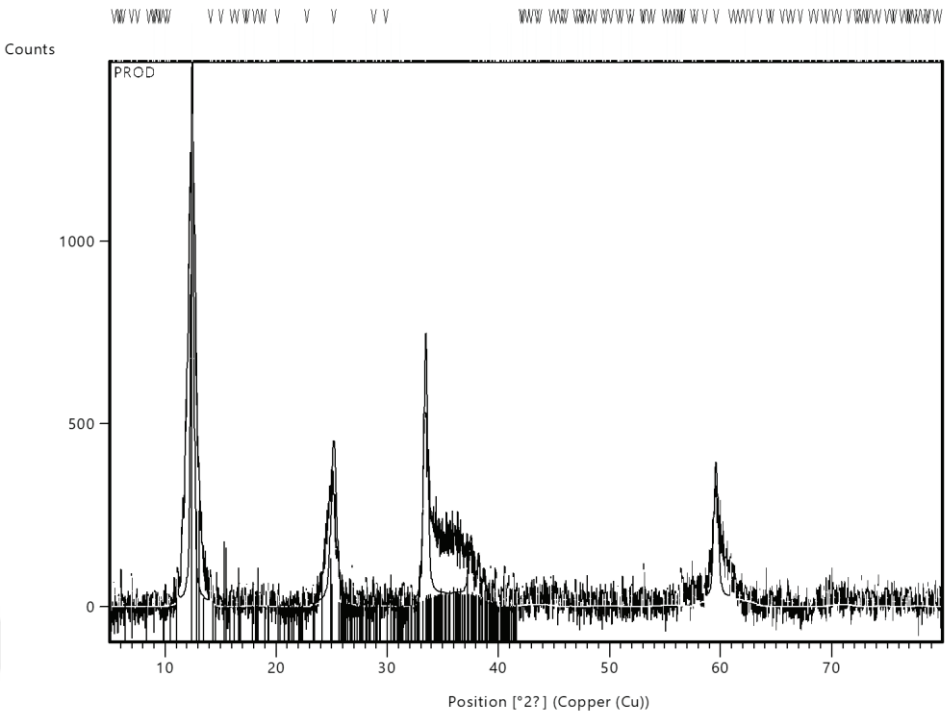

Figure 3.5. Xrd result of $Ni_{0.6}Mn_{0.2}Co_{0.2}(OH)_2$

Since the shoulder structure was not formed in the xrd spectrum of the $Ni_{0.6}Mn_{0.2}Co_{0.2}(OH)_2$ product, it was understood that the structure was beta. Since cobalt and nickel are close elements in the periodic table, it is natural that the xrd peak of this structure resembles the xrd peak of the commercial product. It was observed that the peak intensities increased due to the peaks originating from manganese and the peaks added with cobalt as seen in Figure 3.5.

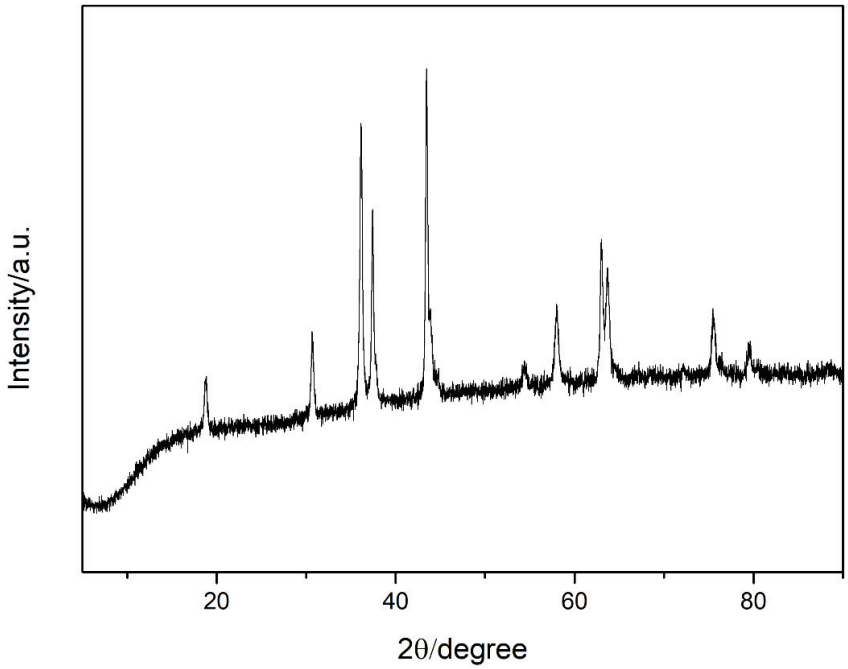

.

Figure 3.6. Xrd result of Al coated $Ni_{0.6}Mn_{0.2}Co_{0.2}(OH)_2$

Shoulder around 10 theta indicates that the aluminum product is alpha structure. Peaks originating from aluminum appear in the xrd spectrum as seen in Figure 3.6.

3. 4. CV Measurements

The impact of reaction time on the electrochemical performances of the as-fabricated $Ni_{0.6}Mn_{0.2}Co_{0.2}(OH)_2$ electrodes was first investigated in a three-electrode system. Cyclic voltammetry (CV) curves of $Ni_{0.6}Mn_{0.2}Co_{0.2}(OH)_2$ electrodes prepared at various reaction times, in which a pair of redox peaks is corresponding to the reversible reactions of

$Ni(OH)_2 + OH^- \rightleftharpoons NiOOH + H_2O + e^-$ and

$Co(OH)_2 + OH^- \rightleftharpoons CoOOH + H_2O + e^-$

Because the oxidation–reduction potentials of Ni^{3+}/Ni^{2+} conversion are higher than those of Co^{3+}/Co^{2+} Conversion a higher Ni/Co ratio results in the shift of CV peaks toward higher potential with the increment of reaction time. More importantly, the CV

area increases first and then declines with the prolonging of treatment time, where the maximum value occurs at 90 min, suggesting that the best electrochemical activity is achieved at this time point. As expected, CV measurements exhibit a similar change tendency and achieves the highest value for the electrode of $Ni_{0.6}Mn_{0.2}Co_{0.2}(OH)_2$. This capacity variation is closely related to the morphological evolution of $Ni_{0.6}Mn_{0.2}Co_{0.2}(OH)_2$ as displayed.

Oxidation and reduction peaks of Ni was observed between ~0.2-0.3 V for every samples. Maximum current value was observed for Al-coated $Ni_{0.6}Mn_{0.2}Co_{0.2}(OH)_2$. Stability measurements of respective powders were measured by using chronoamperometry method. All 3 samples were very stable for 5 h and Al-coated $Ni_{0.6}Mn_{0.2}Co_{0.2}(OH)_2$ showed the maximum current value at given voltage.

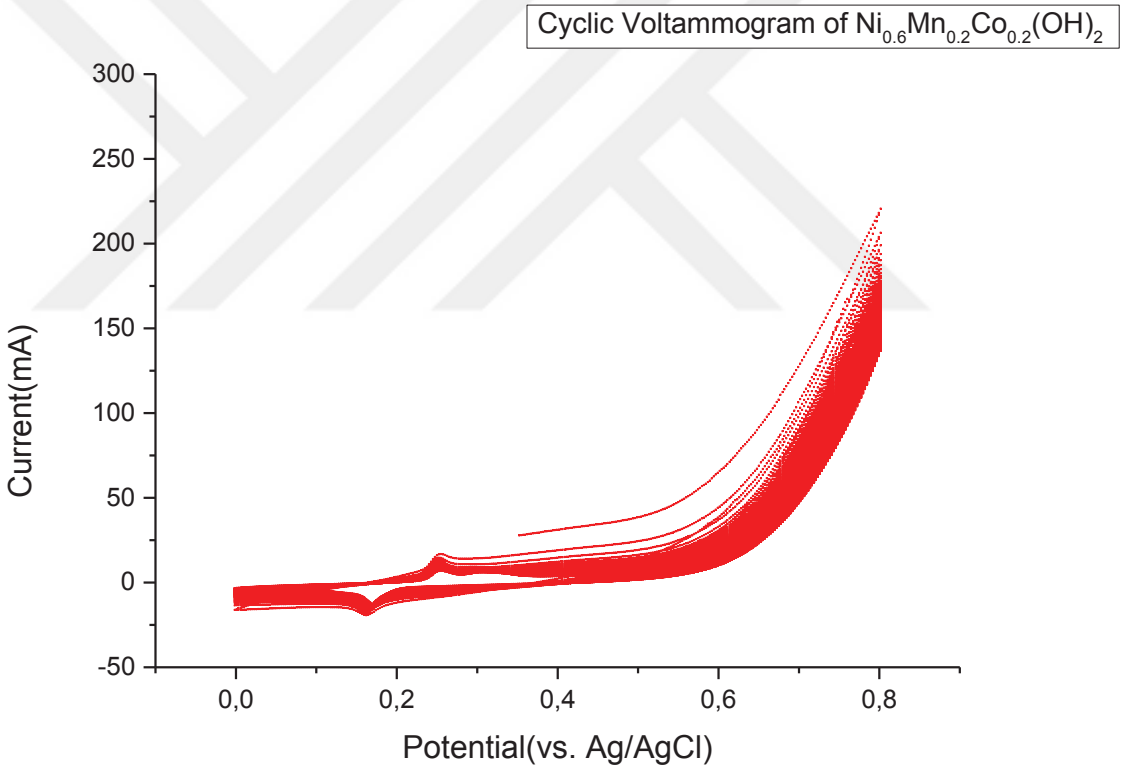

Figure 3.7. Cyclic Voltammogram of $Ni_{0.6}Mn_{0.2}Co_{0.2}(OH)_2$

Cyclic Voltametry measurements were performed using a three-electrode system. Silver/silver chloride was used as the reference electrode. Measurements were made between 0v-0.8v. The maximum current density in the $Ni_{0.6}Mn_{0.2}Co_{0.2}(OH)_2$ was observed to be approximately ~ 206mA. The oxidation and reduction peaks of nickel were observed between 0.15v and 0.26 volts as seen Figure 3.7.

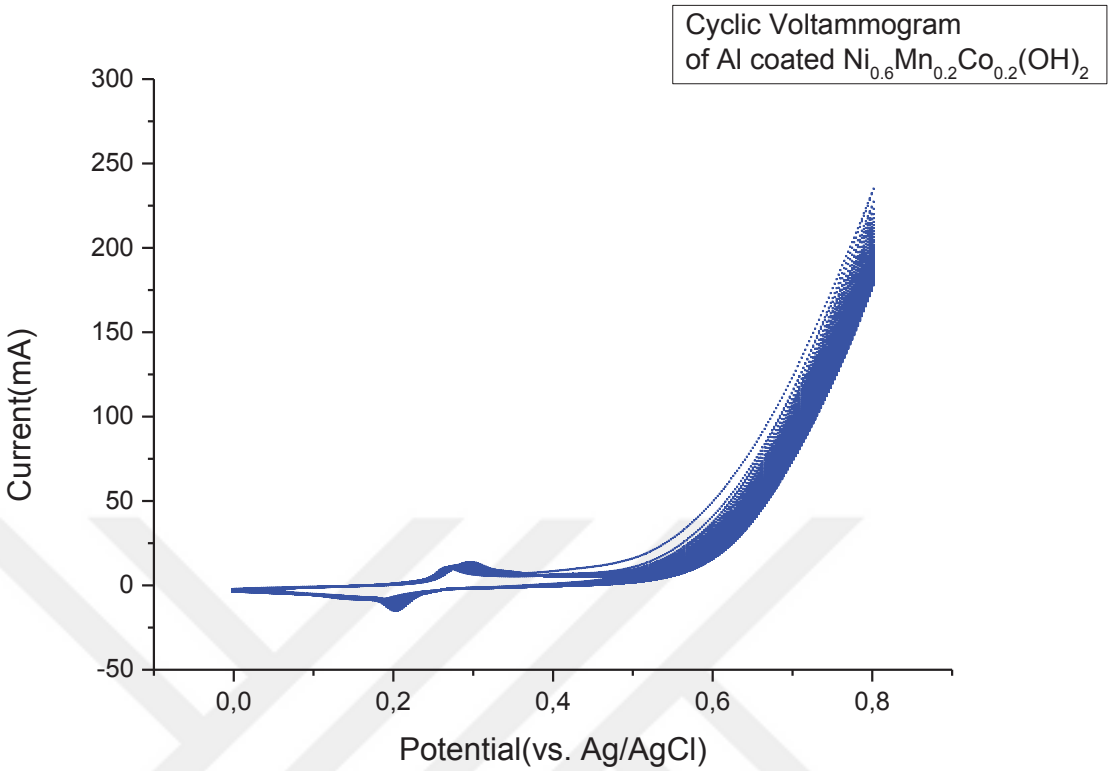

Figure 3.8. Cyclic Voltammogram of Al coated $Ni_{0.6}Mn_{0.2}Co_{0.2}(OH)_2$

Cyclic Voltametry measurements were performed using a three-electrode system. Silver/silver chloride was used as the reference electrode. Measurements were made between 0v-0.8v. The maximum current density in the Al coated $Ni_{0.6}Mn_{0.2}Co_{0.2}(OH)_2$ was observed to be approximately ~ 226mA. The oxidation and reduction peaks of nickel were observed between 0.18v and 0.32 volts as seen Figure 3.8.

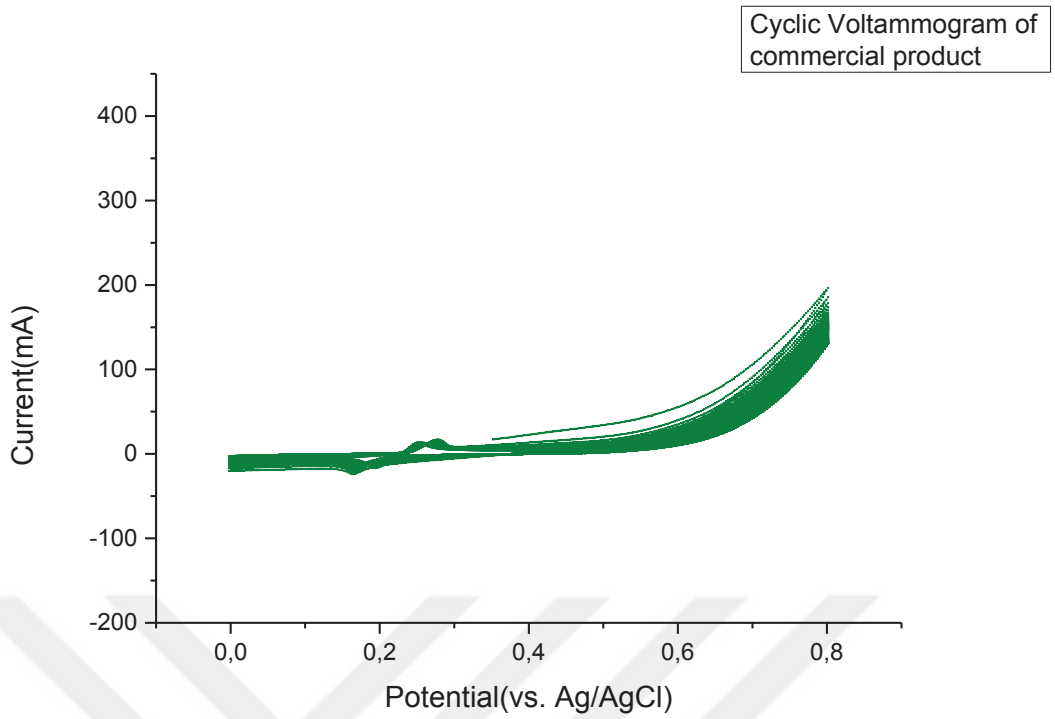

Figure 3.9. Cyclic Voltammogram of commercial product

Cyclic Voltametry measurements were performed using a three-electrode system. Silver/silver chloride was used as the reference electrode. Measurements were made between 0v-0.8v. The maximum current density in the commercial product was observed approximately~ 200mA. The oxidation and reduction peaks of nickel were observed between 0.16v and 0.29 volts as seen Figure 3.9.

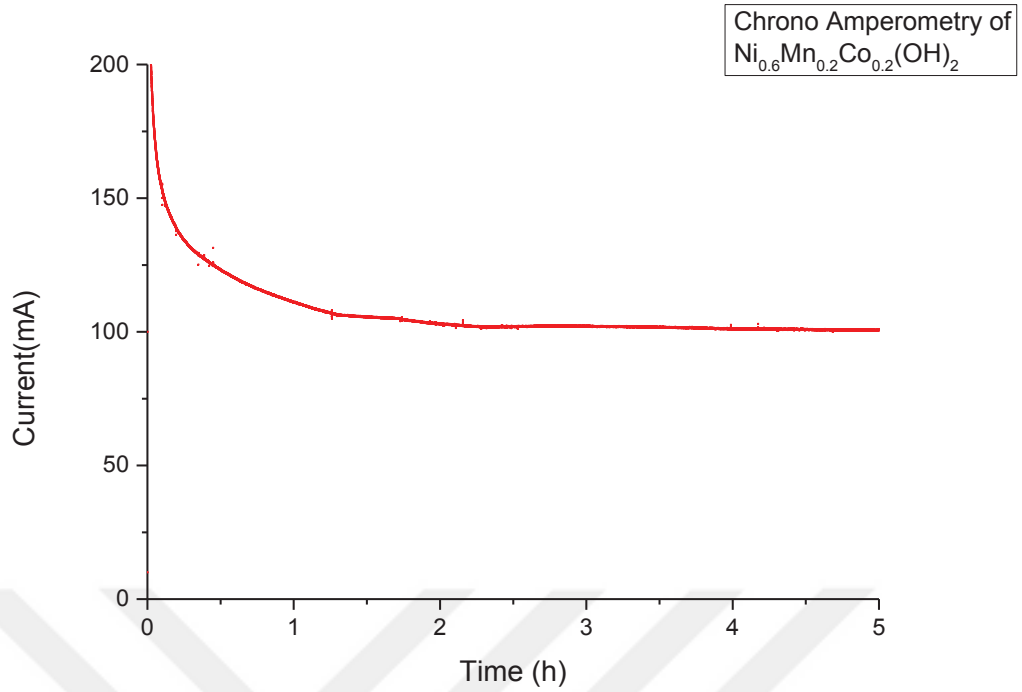

Figure 3.10. Chrono Amperometry of $Ni_{0.6}Mn_{0.2}Co_{0.2}(OH)_2$

Chrono Amperometry measurements were performed using a three-electrode system. Silver/silver chloride was used as the reference electrode. The purpose of this measurement is based on the observation of stability. The measurement took 5 hours. The measurement was carried out in six molar potassium hydroxide. After 5 hours and 100 cycles, the current loss for $Ni_{0.6}Mn_{0.2}Co_{0.2}(OH)_2$ was approximately ~ 33 percent mA as seen in Figure 3.10.

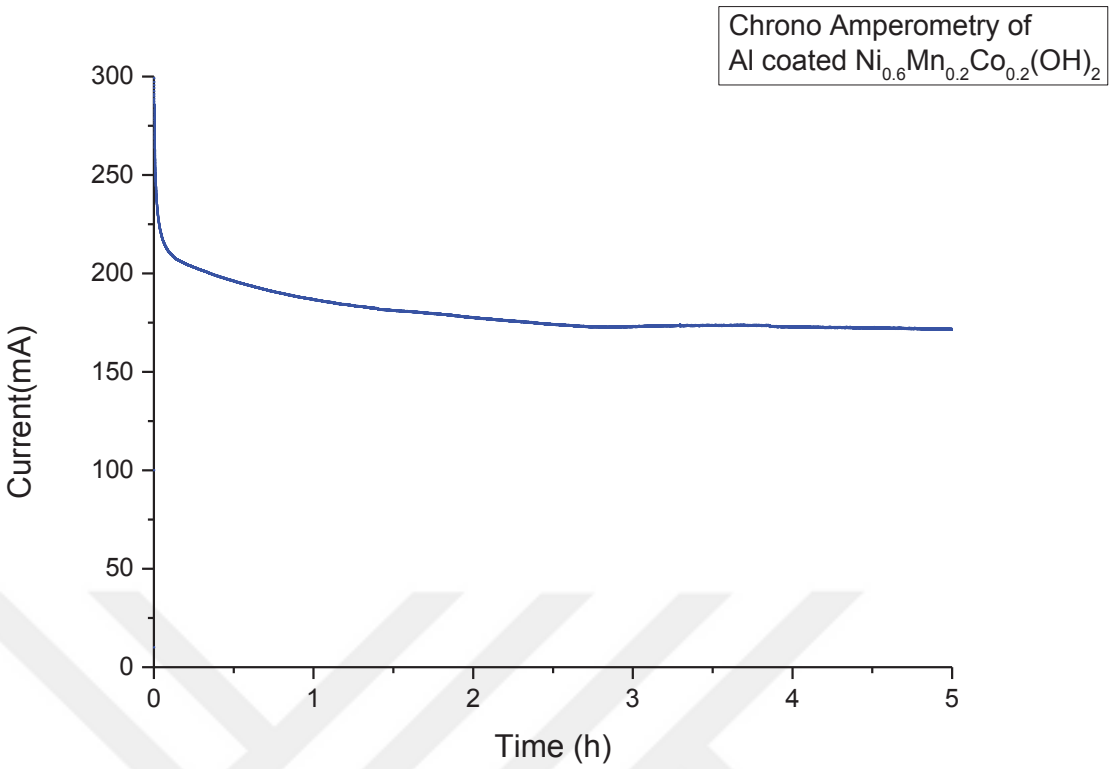

Figure 3.11. Chrono Amperometry of Alcoated $Ni_{0.6}Mn_{0.2}Co_{0.2}(OH)_2$

Chrono Amperometry measurements were performed using a three-electrode system. Silver/silver chloride was used as the reference electrode. The purpose of this measurement is based on the observation of stability. The measurement took 5 hours. The measurement was carried out in six molar potassium hydroxide. After 5 hours and 100 cycles, the current loss for Al coated $Ni_{0.6}Mn_{0.2}Co_{0.2}(OH)_2$ was approximately ~ 18 percent mA as seen in Figure 3.11.

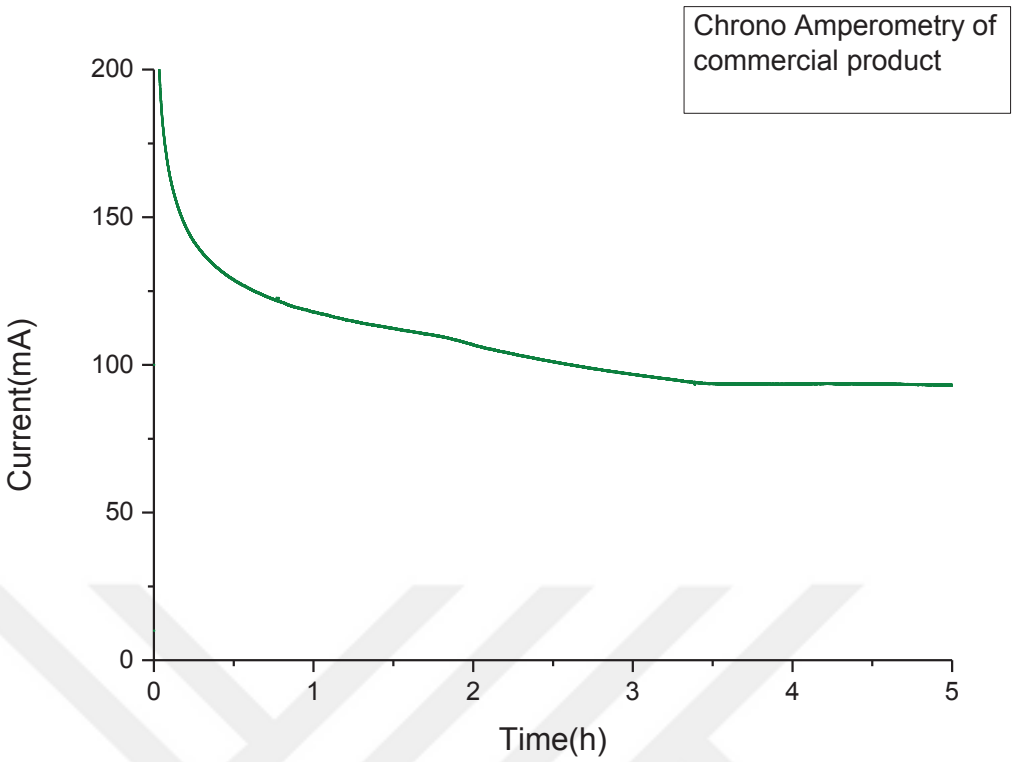

Figure 3.12. Chrono Amperometry of commercial product

Chrono Amperometry measurements were performed using a three-electrode system. Silver/silver chloride was used as the reference electrode. The purpose of this measurement is based on the observation of stability. The measurement took 5 hours. The measurement was carried out in six molar potassium hydroxide. After 5 hours and 100 cycles, the current loss for commercial product was approximately ~ 40 percent mA as seen in Figure 3.12.

CHAPTER 4

CONCLUSION

In this thesis, Al-coated Ni0.6Mn0.2Co0.2(OH)2 powder were produced by urea decomposition method, its effect on electrochemical performance was observed. XRD and SEM analyzes were performed on these samples. As a result of XRD, α- and β-phases of $Ni(OH)_2$, which should be present in the powders, were observed. In particular, extra peaks that was observed at Al-coated $Ni_{0.6}Mn_{0.2}Co_{0.2}(OH)_2$ which is attributed to AlOOH indicates that the Al-coated $Ni_{0.6}Mn_{0.2}Co_{0.2}(OH)_2$ phase is formed. In SEM analysis, it was understood that the particles ranged from 10 to 20 nanometers, and the particle shapes were close to spherical. No significant difference was observed between the SEM images of the samples without surface modification and the samples with AlOOH surface modification lose its spherical shape and some clusters were observed. The produced powders were coated on the aluminum substrate by co-precipitation , and the coated substrates were subjected to electrochemical tests by 3-electrode cells. CV measurements showed that Al-coated $Ni_{0.6}Mn_{0.2}Co_{0.2}(OH)_2$ had highest current density at a specific voltage and very stable for 5 h. The fact that the AlOOH surface modification acts as a protective barrier on the particles prevented the oxidation of the cathode electrolyte interface and the removal of transition metals from the cathode. It also supported the preservation of structural stability. These positive effects of AlOOH surface modification caused the surface modified sample to have highest current density and better stability to the other samples. In the cyclic voltammetry test, the necessary anodic and cathodic peaks were observed. According to all these results, AlOOH surface modification was successful in increasing the electrochemical performance of NCM cathode materials, which is the main purpose of this study, and showed that AlOOH surface modification at low weight percentages can also be efficient.

FUTURE PERPECTIVES

In this study, Ni0.6Mn0.2Co0.2(OH)2 and Al coated Ni0.6Mn0.2Co0.2(OH)2 products were successfully synthesized. Testing the products in a real battery test may yield more realistic results.

In addition, it has been observed that the aluminum coating process extends the life of the structure. Based on this, the performance of the product should be tested in both nickel-based batteries and lithium-based batteries. When the obtained sem images were examined, it was observed that the spherical structure was deteriorated after the aluminum coating process. Future studies are required to increase globality, and the product obtained in this direction promises much better results in the future. In order to achieve these goals, first of all, the synthesis conditions need to be improved. With more detailed studies of the product, the specific capacity on the battery and features such as capacity retention can be improved.

References

Andersson, A. M., D. P. Abraham, R. Haasch, S. MacLaren, J. Liu, and K. Amine. "Surface Characterization of Electrodes from High Power Lithium-Ion Batteries." *Journal of The Electrochemical Society* 149, no. 10 (2002): A1358. https://doi.org/10.1149/1.1505636. http://dx.doi.org/10.1149/1.1505636.

Arikan, M. "Strontium Aluminate Based Phosphorescence Material Synthesis by Solid State Reaction." M.Sc., Istanbul Technical University, 2010.

Armand, M., Gauthier, M., Magnan, J., Ravet, N. . Method for Synthesis of Carbon-Coated Redox Materials with Controlled Size. 2004.

Ates, Mehmet Nurullah, Qingying Jia, Ankita Shah, Ahmed Busnaina, Sanjeev Mukerjee, and K. M. Abraham. "Mitigation of Layered to Spinel Conversion of a Li-Rich Layered Metal Oxide Cathode Material for Li-Ion Batteries." *Journal of The Electrochemical Society* 161, no. 3 (2013/12/23 2013): A290-A301. https://doi.org/10.1149/2.040403jes. http://dx.doi.org/10.1149/2.040403jes.

Bierwagen, Gordon P. "Film Coating Technologies and Adhesion." *Electrochimica Acta* 37, no. 9 (1992/01/01/ 1992): 1471-78. https://doi.org/https://doi.org/10.1016/0013-4686(92)80092-Z. https://www.sciencedirect.com/science/article/pii/001346869280092Z.

Bloom, Ira, Scott A. Jones, Vincent S. Battaglia, Gary L. Henriksen, Jon P. Christophersen, Randy B. Wright, Chinh D. Ho, Jeffrey R. Belt, and Chester G. Motloch. "Effect of Cathode Composition on Capacity Fade, Impedance Rise and Power Fade in High-Power, Lithium-Ion Cells." *Journal of Power Sources* 124, no. 2 (2003/11/24/ 2003): 538-50. https://doi.org/https://doi.org/10.1016/S0378-7753(03)00806-1. https://www.sciencedirect.com/science/article/pii/S0378775303008061.

Brinker, C. J., G. C. Frye, A. J. Hurd, and C. S. Ashley. "Fundamentals of Sol-Gel Dip Coating." *Thin Solid Films* 201, no. 1 (1991/06/05/ 1991): 97-108. https://doi.org/https://doi.org/10.1016/0040-6090(91)90158-T. https://www.sciencedirect.com/science/article/pii/004060909190158T.

Brinkhaus, Linda. "Degradation Phenomena of Lithium-Rich Lithium-Nickel-Cobalt-Manganese-Oxide in Lithium-Ion-Batteries

Degradationsphänomene Von Lithium-Reichem Lithium-Nickel-Cobalt-Mangan-Oxid in Lithium-Ionen-Batterien." 2015. https://opus4.kobv.de/opus4-fau/frontdoor/index/index/docId/5926

https://nbn-resolving.org/urn:nbn:de:bvb:29-opus4-59269.

"Types of Battery Cells." 2012, http://batteryuniversity.com/learn/article/types_of_battery_cells.

Chen, Zonghai, Dong-Ju Lee, Yang-Kook Sun, and Khalil Amine. "Advanced Cathode Materials for Lithium-Ion Batteries." *MRS Bulletin* 36, no. 7 (2011/07/01 2011): 498-505. https://doi.org/10.1557/mrs.2011.155. https://doi.org/10.1557/mrs.2011.155.

Choi, Ji-won, and Jae-won Lee. "Improved Electrochemical Properties of Li(Ni0.6mn0.2co0.2)O2 by Surface Coating with Li1.3al0.3ti1.7(Po4)3." *Journal of Power Sources* 307 (2016/03/01/ 2016): 63-68. https://doi.org/https://doi.org/10.1016/j.jpowsour.2015.12.055. https://www.sciencedirect.com/science/article/pii/S0378775315306674.

Chung, Sung-Yoon, Jason T. Bloking, and Yet-Ming Chiang. "Electronically Conductive Phospho-Olivines as Lithium Storage Electrodes." *Nature Materials* 1, no. 2 (2002/10/01 2002): 123-28. https://doi.org/10.1038/nmat732. https://doi.org/10.1038/nmat732.

Daniel, Claus, Debasish Mohanty, Jianlin Li, and David L. Wood. "Cathode Materials Review." *AIP Conference Proceedings* 1597, no. 1 (2014/06/16 2014): 26-43. https://doi.org/10.1063/1.4878478. https://aip.scitation.org/doi/abs/10.1063/1.4878478.

Darab, M. "Synthesis and Characterşzatşon of Nanostructured Cathode Material(Bscf) for Solid Oxide Fuel Cells." M.Sc, Royal Institute of Technology, 2010.

de las Casas, Charles, and Wenzhi Li. "A Review of Application of Carbon Nanotubes for Lithium Ion Battery Anode Material." *Journal of Power Sources* 208 (2012/06/15/ 2012): 74-85. https://doi.org/https://doi.org/10.1016/j.jpowsour.2012.02.013. https://www.sciencedirect.com/science/article/pii/S037877531200314X.

Delacourt, C., L. Laffont, R. Bouchet, C. Wurm, J. B. Leriche, M. Morcrette, J. M. Tarascon, and C. Masquelier. "Toward Understanding of Electrical Limitations (Electronic, Ionic) in Limpo[Sub 4] (M=Fe, Mn) Electrode Materials." *Journal of*

The Electrochemical Society 152, no. 5 (2005): A913. https://doi.org/10.1149/1.1884787. http://dx.doi.org/10.1149/1.1884787.

Demiray, M. "Synthesis and Characterization of Some Metal Oxide Containing Compounds." M.Sc., Erciyes University, 2007.

Denizli, F. "Physical Vapor with Electron Beam for Lithium-ıon Batteries Production and Characterization of Thin Film Anode Material Using Deposition Method." M.Sc., Istanbul Technical University 2011.

Eker, E. "Solid State Synthesis and Characterization of Lanthanborate Compound." M.Sc, Hacettepe University, 2006.

Endo, M., C. Kim, K. Nishimura, T. Fujino, and K. Miyashita. "Recent Development of Carbon Materials for Li Ion Batteries." *Carbon* 38, no. 2 (2000/01/01/ 2000): 183-97. https://doi.org/https://doi.org/10.1016/S0008-6223(99)00141-4. https://www.sciencedirect.com/science/article/pii/S0008622399001414.

Goodenough, John B., and Youngsik Kim. "Challenges for Rechargeable Li Batteries." *Chemistry of Materials* 22, no. 3 (2010/02/09 2010): 587-603. https://doi.org/10.1021/cm901452z. https://doi.org/10.1021/cm901452z.

He, Huibing, Ling Zan, and Youxiang Zhang. "Effects of Amorphous V2o5 Coating on the Electrochemical Properties of Li[Li0.2mn0.54ni0.13co0.13]O2 as Cathode Material for Li-Ion Batteries." *Journal of Alloys and Compounds* 680 (2016/09/25/ 2016): 95-104. https://doi.org/https://doi.org/10.1016/j.jallcom.2016.04.115. https://www.sciencedirect.com/science/article/pii/S0925838816310799.

He, Wei, Dingding Yuan, Jiangfeng Qian, Xinping Ai, Hanxi Yang, and Yuliang Cao. "Enhanced High-Rate Capability and Cycling Stability of Na-Stabilized Layered Li1.2[Co0.13ni0.13mn0.54]O2 Cathode Material." 10.1039/C3TA12296D. *Journal of Materials Chemistry A* 1, no. 37 (2013): 11397-403. https://doi.org/10.1039/C3TA12296D. http://dx.doi.org/10.1039/C3TA12296D.

"Http://Www.Emc2.Cornell.Edu/Content/View/Battery-Anodes.Html." accessed 03.08, 2021, http://www.emc2.cornell.edu/content/view/battery-anodes.html.

"Http://Www.Epectec.Com/Batteries/Cell-Comparison.Html." accessed 02.24, 2021, http://www.epectec.com/batteries/cell-comparison.html.

"Http://Www.Lehigh.Edu/Imi/Teched/Lecbasic/Marques_Sol_Gel.Pdf." accessed 03.20, 2021, http://www.lehigh.edu/imi/teched/LecBasic/Marques_Sol_gel.pdf.

"Http://Www.Mtixtl.Com/Micrometeradjustablefilmapplicator-250mmeq-Se-Ktq-250.Aspx." accessed 04.03, 2021, http://www.mtixtl.com/MicrometerAdjustableFilmApplicator-250mmEQ-Se-KTQ-250.aspx.

, accessed 03.03, 2021, http://www.pasticheenergysolutions.com/applications/.

"Http://Www.Sneresearch.Com/Eng/Info/Show.Php?C_Id=4970&Pg=5&S_Sort=&Sub_Ca T=&S_Type=&S_Word= ", accessed 03.22, 2021, http://www.sneresearch.com/eng/info/show.php?c_id=4970&pg=5&s_sort=&sub_ca t=&s_type=&s_word=

Hu, Meng, Xiaoli Pang, and Zhen Zhou. "Recent Progress in High-Voltage Lithium Ion Batteries." *Journal of Power Sources* 237 (2013/09/01/ 2013): 229-42. https://doi.org/https://doi.org/10.1016/j.jpowsour.2013.03.024. https://www.sciencedirect.com/science/article/pii/S0378775313004059.

Hummel, R. E. . *Properties of Materials.* New York: Springer, 2011.

Inoue, N., and Y. Zou. "Electronic Structure and Lithium Ion Migration of La4/3−Yli3yti2o6 Using Cluster Model." *Solid State Ionics* 176, no. 31 (2005/10/01/ 2005): 2341-44. https://doi.org/https://doi.org/10.1016/j.ssi.2005.01.013. https://www.sciencedirect.com/science/article/pii/S0167273805002833.

Jin, Xue, Qunjie Xu, Haimei Liu, Xiaolei Yuan, and Yongyao Xia. "Excellent Rate Capability of Mg Doped Li[Li0.2ni0.13co0.13mn0.54]O2 Cathode Material for Lithium-Ion Battery." *Electrochimica Acta* 136 (2014/08/01/ 2014): 19-26. https://doi.org/https://doi.org/10.1016/j.electacta.2014.05.043. https://www.sciencedirect.com/science/article/pii/S0013468614010275.

Jin, Yanling, Youlong Xu, Xiaofei Sun, Lilong Xiong, and Shengchun Mao. "Electrochemically Active Mno2 Coated Li1.2ni0.18co0.04mn0.58o2 Cathode with Highly Improved Initial Coulombic Efficiency." *Applied Surface Science* 384 (2016/10/30/ 2016): 125-34. https://doi.org/https://doi.org/10.1016/j.apsusc.2016.04.136. https://www.sciencedirect.com/science/article/pii/S0169433216309199.

Johnson, C. S., J. S. Kim, C. Lefief, N. Li, J. T. Vaughey, and M. M. Thackeray. "The Significance of the Li2mno3 Component in 'Composite' Xli2mno3·(1−X)Limn0.5ni0.5o2 Electrodes." *Electrochemistry Communications* 6, no. 10 (2004/10/01/ 2004): 1085-91.

https://doi.org/https://doi.org/10.1016/j.elecom.2004.08.002. https://www.sciencedirect.com/science/article/pii/S1388248104002127.

Kakihana, Masato, and Masahiro Yoshimura. "Synthesis and Characteristics of Complex Multicomponent Oxides Prepared by Polymer Complex Method." *Bulletin of the Chemical Society of Japan* 72, no. 7 (1999/07/01 1999): 1427-43. https://doi.org/10.1246/bcsj.72.1427. https://doi.org/10.1246/bcsj.72.1427.

Kang, Sun-Ho, John B. Goodenough, and Llewellyn K. Rabenberg. "Effect of Ball-Milling on 3-V Capacity of Lithium−Manganese Oxospinel Cathodes." *Chemistry of Materials* 13, no. 5 (2001/05/01 2001): 1758-64. https://doi.org/10.1021/cm000920g. https://doi.org/10.1021/cm000920g.

Kong, Ji-Zhou, Chong Ren, Guo-An Tai, Xiang Zhang, Ai-Dong Li, Di Wu, Hui Li, and Fei Zhou. "Ultrathin Zno Coating for Improved Electrochemical Performance of Lini0.5co0.2mn0.3o2 Cathode Material." *Journal of Power Sources* 266 (2014/11/15/ 2014): 433-39. https://doi.org/https://doi.org/10.1016/j.jpowsour.2014.05.027. https://www.sciencedirect.com/science/article/pii/S0378775314007095.

Kong, Ji-Zhou, Shan-Shan Wang, Guo-An Tai, Lin Zhu, Lai-Guo Wang, Hai-Fa Zhai, Di Wu, Ai-Dong Li, and Hui Li. "Enhanced Electrochemical Performance of Lini0.5co0.2mn0.3o2 Cathode Material by Ultrathin Zro2 Coating." *Journal of Alloys and Compounds* 657 (2016/02/05/ 2016): 593-600. https://doi.org/https://doi.org/10.1016/j.jallcom.2015.10.187. https://www.sciencedirect.com/science/article/pii/S0925838815314432.

Leclanche, G. . "New Form of Galvanic Battery." *Comptes Rendus Chimie* 83 (1866): 54-56.

Li, Bing, Jing Wang, Zulai Cao, Peng Zhang, and Jinbao Zhao. "The Role of Sno2 Surface Coating in the Electrochemical Performance of Li1.2mn0.54co0.13ni0.13o2 Cathode Materials." *Journal of Power Sources* 325 (2016/09/01/ 2016): 84-90. https://doi.org/https://doi.org/10.1016/j.jpowsour.2016.06.027. https://www.sciencedirect.com/science/article/pii/S0378775316307297.

Li, Qi, Guangshe Li, Chaochao Fu, Dong Luo, Jianming Fan, and Liping Li. "K+-Doped Li1.2mn0.54co0.13ni0.13o2: A Novel Cathode Material with an Enhanced Cycling Stability for Lithium-Ion Batteries." *ACS Applied Materials & Interfaces* 6, no. 13 (2014/07/09 2014): 10330-41. https://doi.org/10.1021/am5017649. https://doi.org/10.1021/am5017649.

Linden, D. Reddy, T. B. (Ed.). . *Handbook of Batteries*. 3 ed. New York: McGraw-Hill, 2002.

Liu, W., G. C. Farrington, F. Chaput, and B. Dunn. "Synthesis and Electrochemical Studies of Spinel Phase Limn2 O 4 Cathode Materials Prepared by the Pechini Process." *Journal of The Electrochemical Society* 143, no. 3 (1996/03/01 1996): 879-84. https://doi.org/10.1149/1.1836552. http://dx.doi.org/10.1149/1.1836552.

Lu, Huaquan, Haitao Zhou, Ann Mari Svensson, Anita Fossdal, Edel Sheridan, Shigang Lu, and Fride Vullum-Bruer. "High Capacity Li[Ni0.8co0.1mn0.1]O2 Synthesized by Sol–Gel and Co-Precipitation Methods as Cathode Materials for Lithium-Ion Batteries." *Solid State Ionics* 249-250 (2013/11/01/ 2013): 105-11. https://doi.org/https://doi.org/10.1016/j.ssi.2013.07.023. https://www.sciencedirect.com/science/article/pii/S0167273813003548.

Mizushima, K., P. C. Jones, P. J. Wiseman, and J. B. Goodenough. "Lixcoo2 (0<X<-1): A New Cathode Material for Batteries of High Energy Density." *Materials Research Bulletin* 15, no. 6 (1980/06/01/ 1980): 783-89. https://doi.org/https://doi.org/10.1016/0025-5408(80)90012-4. https://www.sciencedirect.com/science/article/pii/0025540880900124.

Nitta, Naoki, Feixiang Wu, Jung Tae Lee, and Gleb Yushin. "Li-Ion Battery Materials: Present and Future." *Materials Today* 18, no. 5 (2015/06/01/ 2015): 252-64. https://doi.org/https://doi.org/10.1016/j.mattod.2014.10.040. https://www.sciencedirect.com/science/article/pii/S1369702114004118.

Okada, Shigeto, Shoichiro Sawa, Minato Egashira, Jun-ichi Yamaki, Mitsuharu Tabuchi, Hiroyuki Kageyama, Tokuzo Konishi, and Akira Yoshino. "Cathode Properties of Phospho-Olivine Limpo4 for Lithium Secondary Batteries." *Journal of Power Sources* 97-98 (2001/07/01/ 2001): 430-32. https://doi.org/https://doi.org/10.1016/S0378-7753(01)00631-0. https://www.sciencedirect.com/science/article/pii/S0378775301006310.

Oljaca, Miodrag, Berislav Blizanac, Aurelien Du Pasquier, Yipeng Sun, Ranko Bontchev, Arek Suszko, Ryan Wall, and Kenneth Koehlert. "Novel Li(Ni1/3co1/3mn1/3)O2 Cathode Morphologies for High Power Li-Ion Batteries." *Journal of Power Sources* 248 (2014/02/15/ 2014): 729-38. https://doi.org/https://doi.org/10.1016/j.jpowsour.2013.09.102. https://www.sciencedirect.com/science/article/pii/S037877531301608X.

Orendorff, C. J., and D. H. Doughty. "Lithium Ion Battery Safety." *Interface magazine* 21, no. 2 (2012/01/01 2012): 35-35. https://doi.org/10.1149/2.f02122if. http://dx.doi.org/10.1149/2.F02122if.

Pan, Cheng-chi, Yi-rong Zhu, Ying-chang Yang, Hong-shuai Hou, Ming-jun Jing, Wei-xin Song, Xu-ming Yang, and Xiao-bo Ji. "Influences of Transition Metal on Structural and Electrochemical Properties of Li[Nixcoymnz]O2 (0.6≤X≤0.8) Cathode Materials for Lithium-Ion Batteries." *Transactions of Nonferrous Metals Society of China* 26, no. 5 (2016/05/01/ 2016): 1396-402. https://doi.org/https://doi.org/10.1016/S1003-6326(16)64244-9. https://www.sciencedirect.com/science/article/pii/S1003632616642449.

Pillot, C. "Micro Hybrid, Hev, P-Hev and Ev Market 2012–2025 Impact on the Battery Business." Paper presented at the 2013 World Electric Vehicle Symposium and Exhibition (EVS27), 17-20 Nov. 2013 2013.

Reed, J., G. Ceder, and A. Van Der Ven. "Layered-to-Spinel Phase Transition in Li[Sub X]Mno[Sub 2]." *Electrochemical and Solid-State Letters* 4, no. 6 (2001): A78. https://doi.org/10.1149/1.1368896. http://dx.doi.org/10.1149/1.1368896.

Rehg, Timothy J., and G. Higgins. "Spin Coating of Colloidal Suspensions." https://doi.org/10.1002/aic.690380403. *AIChE Journal* 38, no. 4 (1992/04/01 1992): 489-501. https://doi.org/https://doi.org/10.1002/aic.690380403. https://doi.org/10.1002/aic.690380403.

Rozier, Patrick, and Jean Marie Tarascon. "Review—Li-Rich Layered Oxide Cathodes for Next-Generation Li-Ion Batteries: Chances and Challenges." *Journal of The Electrochemical Society* 162, no. 14 (2015): A2490-A99. https://doi.org/10.1149/2.0111514jes. http://dx.doi.org/10.1149/2.0111514jes.

Shi, S. J., J. P. Tu, Y. J. Zhang, Y. D. Zhang, X. Y. Zhao, X. L. Wang, and C. D. Gu. "Effect of Sm2o3 Modification on Li[Li0.2mn0.56ni0.16co0.08]O2 Cathode Material for Lithium Ion Batteries." *Electrochimica Acta* 108 (2013/10/01/ 2013): 441-48. https://doi.org/https://doi.org/10.1016/j.electacta.2013.07.020. https://www.sciencedirect.com/science/article/pii/S0013468613012899.

Shukla, A. K., Kumar, T. P. "Materials for Next Generation Lithium Batteries." *Current Science* 94 (2008): 317-27.

Volta, A. "On the Electricity Excited by the Mere Contact of Conducting Substances of Different Kinds. In a Letter from Mr. Alexander Volta, Frs Professor of Natural

Philosophy in the University of Pavia, to the Rt. Hon. Sir Joseph Banks, Bart. Kbprs.". *Royal Society of London* (1800): 403-31.

Wang, Haiyan, Aidong Tang, and Kelong Wang. "Thermal Behavior Investigation of Lini1/3co1/3mn1/3o2-Based Li-Ion Battery under Overcharged Test." https://doi.org/10.1002/cjoc.201190056. *Chinese Journal of Chemistry* 29, no. 1 (2011/01/01 2011): 27-32. https://doi.org/https://doi.org/10.1002/cjoc.201190056. https://doi.org/10.1002/cjoc.201190056.

Wohlfahrt-Mehrens, M., C. Vogler, and J. Garche. "Aging Mechanisms of Lithium Cathode Materials." *Journal of Power Sources* 127, no. 1 (2004/03/10/ 2004): 58-64. https://doi.org/https://doi.org/10.1016/j.jpowsour.2003.09.034. https://www.sciencedirect.com/science/article/pii/S0378775303009376.

Wu, Y., and A. Manthiram. "Effect of Surface Modifications on the Layered Solid Solution Cathodes (1−Z) Li[Li1/3mn2/3]O2−(Z) Li[Mn0.5−Yni0.5−Yco2y]O2." *Solid State Ionics* 180, no. 1 (2009/02/16/ 2009): 50-56. https://doi.org/https://doi.org/10.1016/j.ssi.2008.11.002. https://www.sciencedirect.com/science/article/pii/S0167273808006437.

Xu, Bo, Danna Qian, Ziying Wang, and Ying Shirley Meng. "Recent Progress in Cathode Materials Research for Advanced Lithium Ion Batteries." *Materials Science and Engineering: R: Reports* 73, no. 5 (2012/05/01/ 2012): 51-65. https://doi.org/https://doi.org/10.1016/j.mser.2012.05.003. https://www.sciencedirect.com/science/article/pii/S0927796X12000186.

Yao, Fei, and Costel Sorin Cojocaru. "Carbon-Based Nanomaterials as an Anode for Lithium Ion Battery." Ecole Polytechnique X, 2013. https://pastel.archives-ouvertes.fr/pastel-00967913.

Yu, Haijun, Hyunjeong Kim, Yarong Wang, Ping He, Daisuke Asakura, Yumiko Nakamura, and Haoshen Zhou. "High-Energy 'Composite' Layered Manganese-Rich Cathode Materials Via Controlling Li2mno3 Phase Activation for Lithium-Ion Batteries." 10.1039/C2CP40745K. *Physical Chemistry Chemical Physics* 14, no. 18 (2012): 6584-95. https://doi.org/10.1039/C2CP40745K. http://dx.doi.org/10.1039/C2CP40745K.

Yuan, J., Liu, X., and Zhang, H. (Ed.). . *Lithium-Ion Batteries: Advanced Materials and Technologies.* Vol. 7, USA: CRC Press, 2013.

Zhang, Wei-Jun. "A Review of the Electrochemical Performance of Alloy Anodes for Lithium-Ion Batteries." *Journal of Power Sources* 196, no. 1 (2011/01/01/ 2011): 13-24. https://doi.org/https://doi.org/10.1016/j.jpowsour.2010.07.020. https://www.sciencedirect.com/science/article/pii/S0378775310011699.

———. "Structure and Performance of Lifepo4 Cathode Materials: A Review." *Journal of Power Sources* 196, no. 6 (2011/03/15/ 2011): 2962-70. https://doi.org/https://doi.org/10.1016/j.jpowsour.2010.11.113. https://www.sciencedirect.com/science/article/pii/S037877531002104X.

Zhou, Lin, Mijie Tian, Yunlong Deng, Qiaoji Zheng, Chenggang Xu, and Dunmin Lin. "La2o3-Coated Li1.2mn0.54ni0.13co0.13o2 as Cathode Materials with Enhanced Specific Capacity and Cycling Stability for Lithium-Ion Batteries." *Ceramics International* 42, no. 14 (2016/11/01/ 2016): 15623-33. https://doi.org/https://doi.org/10.1016/j.ceramint.2016.07.016. https://www.sciencedirect.com/science/article/pii/S0272884216310732.

Zhou, Yanke, Peifeng Bai, Haoqing Tang, Jiangtao Zhu, and Zhiyuan Tang. "Chemical Deposition Synthesis of Desirable High-Rate Capability Al2o3-Coated Li1.2mn0.54ni0.13co0.13o2 as a Lithium Ion Battery Cathode Material." *Journal of Electroanalytical Chemistry* 782 (2016/12/01/ 2016): 256-63. https://doi.org/https://doi.org/10.1016/j.jelechem.2016.10.049. https://www.sciencedirect.com/science/article/pii/S1572665716305914.